Journal of Computational Physics **153,** 225–272 (1999)
Article ID jcph.1999.6287, available online at http://www.idealibrary.com on IDEAL®

REVIEW

Basics of Surface Hopping in Mixed Quantum/Classical Simulations

Karen Drukker[1]

Universiteit van Amsterdam, Amsterdam, The Netherlands, and University of Notre Dame, Notre Dame, Indiana
E-mail: karen@chem.nwu.edu

Received September 25, 1998; revised May 5, 1999

This paper gives an overview of mixed quantum/classical simulation techniques based on the ideas of surface hopping (Tully, 1990). Basics such as the separation of a system into a classical and a quantum mechanical part are addressed. First, the Ehrenfest approach, which relies on a single-configuration approximation to the total wave function, is explained. Then an analogous multi-configurational approach, to which surface hopping is an approximation, is given. The surface hopping method developed by John Tully is explained in detail. Several other methods are summarized and applications are discussed briefly to illustrate the scope of these methods.

1. INTRODUCTION

Computer simulations have contributed significantly to the understanding of many chemical, physical, and biochemical phenomena. Some types of simulation provide information on static or equilibrium properties of a system only, but other methods, such as molecular dynamics, directly mimic real-time dynamics so that dynamical processes can be studied in detail. The latter class of simulations is our main interest in this paper. Molecular dynamics simulations have been done at many "levels," ranging from *ab initio* simulations to entirely classical simulations. Many of the systems of interest are large because most reactions take place in solution. Quantum effects play a significant role in many of these reactions. It is quite a challenge to simulate such systems because on the one hand all interactions within the system have to be incorporated, while on the other hand the significant quantum effects have to be accounted for as well.

[1]Current address: Northwestern University, Evanston, IL.

0021-9991/99 $30.00

The most ambitious approach is to treat the entire system quantum mechanically. Currently, however, exact quantum dynamical simulations are restricted to dealing with small systems on short time scales because of the formidable computational cost involved. The most straightforward approach, on the other hand, is to neglect quantum effects or to include them in some effective way and then treat the entire system classically. Classical simulations are conceptually simple. If one knows how the particles in the system interact, one can compute the forces between them and solve Newton's equations of motion to propagate the system in discrete time. This is straightforward and computationally cheap (compared to doing quantum calculations). Dynamics can be investigated over long time scales and, moreover, relatively large systems can be studied. Although patience is still a virtue, nowadays a classical simulation can easily cover the nanosecond range time scale while dealing with a system of on the order of 10,000 atoms or even more (see, for a recent example, Ref. [2]). Obviously simulation within the classical limit is the method of choice for a large number of systems. Modeling interactions between particles remains a challenge, however. This can be illustrated, for instance, by the multitude of available potential models for simulation of bulk water (to name a very few [3–5]).

If quantum effects are known to be important, modeling the system within a classical treatment fails to accurately reproduce experimentally observed quantities. A compromise between an entirely quantum mechanical treatment and a completely classical one is simulation within a mixed quantum/classical framework. The quantum character of a few selected degrees of freedom is included explicitly while the remainder of the system is treated classically. An advantage is that a larger—although mainly classical—system can be studied while the "most important" quantum effects are incorporated. Separation of the total system in a classical part and a quantum mechanical part is not trivial since classical and quantum dynamics are incompatible in principle. A key issue is self-consistency. The degrees of freedom that are treated quantum mechanically must evolve correctly under influence of the classical degrees of freedom, while the motion of the classical degrees of freedom in turn must depend correctly on that of the quantum degrees of freedom. An accurate treatment of this latter feedback is especially challenging. There are a number of standard approaches to describe the dynamics of the quantum degrees of freedom under the influence of classical degrees of freedom, such as the classical path method [6]. This method, however, fails to include the influence of the quantum dynamics on the dynamics of the classical system. In this paper we discuss two classes of methods that attempt to treat the quantum and classical degrees of freedom in a self-consistent way. The first class of methods is based on a mean field treatment (see, e.g., Ref. [7]) (Section 2.1) and the second one is surface hopping [1] (Section 2.7). Depending on the mixed quantum/classical method of choice and the complexity of the system typically dynamics can be studied over a range of a few tens of femtoseconds to a few hundred picoseconds. The longer time scales are possible for simulations in which the quantum dynamics is adiabatic, i.e., when the Born–Oppenheimer approximation is valid. Then the quantum subsystem adjusts itself infinitely fast to the motion of the classical particles and remains in its initial state. The number of degrees of freedom that can be treated quantum mechanically may be limited, especially for methods based on wave functions, and the memory requirements for large-scale applications may increase dramatically.

In this paper an introduction to wave function-based methods is given [8]. Methods based on path integrals [9–20], which are widely used for incorporation of quantum effects, are not discussed, however. Path integral methods are very well suited to the study of structural

or equilibrium properties of a system or, in combination with transition state theory, to the calculation of rate constants. A disadvantage is that it is generally much harder to extract real-time dynamical properties [21, 22]. A notable exception in that respect is centroid molecular dynamics [23–30], a promising method based on the centroid variable in the path integral formulation [9]. An advantage of path integral-based methods over wave function-based methods is that often many more degrees of freedom can be treated quantum mechanically.

In the methods discussed in this paper the system is separated in a strictly classical part and a quantum mechanical part, although some of the derivations rely on a semiclassical formulation. Nuclear quantum effects such as tunneling are not incorporated at all or at best are treated in a phenomenological manner. Semiclassical methods or mixed quantum/semiclassical methods are not discussed. Recent developments in this area [31–37] are very promising for dealing with the kind of systems discussed in this paper. Also, this paper deals exclusively with methods in which interactions in the system are modeled in advance. This obviously introduces approximations and inaccuracies. A method that does not rely on preassigned interaction potentials is the Car–Parrinello simulation method [38, 39]. Here the forces are determined on the fly from electronic structure calculations. Car–Parrinello is typically used for classical dynamics (see, e.g., [40–42]), although recently it has been combined with path integral methods in order to incorporate quantum effects [43], and is generally limited to systems of a small number of molecules.

The outline of this paper is as follows. The Introduction briefly summarizes the molecular dynamics method and properties that are generally of interest in this kind of simulation. Section 2 explains the basic ideas of mixed quantum/classical simulations. First, the separation of the system into "fast" (quantum mechanical) and "slow" (classical) degrees of freedom is explained within a mean field treatment. Then several issues such as the adiabatic, or Born–Oppenheimer, approximation and the interaction between quantum and classical degrees of freedom are discussed. Second, it is shown that the separation of degrees of freedom for surface hopping methods can be obtained analogously to the mean field case. The "molecular dynamics with quantum transitions" surface hopping method is discussed in detail. Limitations of both mean field methods and surface hopping methods are mentioned in the course of this section. The subsequent two sections deal with more "sophisticated" methods. The first summarizes a method for the study of infrequent events (Section 3). The second describes a method with which to calculate quantum wave functions for more than a single quantum degree of freedom (Section 4). Each section includes an application as an illustration of the methods discussed. We conclude in Section 5.

1.1. *Classical and Quantum Molecular Dynamics*

A thorough review of classical simulation techniques can be found in Allen and Tildesley [44] and a more recent book by Smit and Frenkel [45]. An experimental condensed phase system that contains on the order of $>10^{23}$ particles is often modeled with a limited number of particles within a volume, which is called the simulation box. Often periodic boundaries of the simulation box are applied in order to mimic an infinitely large system. In general one would like to choose a system as small as possible (because that is cheap computationally speaking) while avoiding finite size effects, i.e., artifacts, due to an insufficiently large system. Since mixed quantum/classical simulations are more computationally expensive than classical ones it is even more crucial to balance cost against the likelihood of artifacts.

The interaction between atoms is governed by their internal electronic structure. In simulations based on *a priori* modeled interactions each atom type has a specific interaction potential. A common way to simplify the calculation of the total potential energy is to approximate it with a sum over pairwise interactions dependent on the interatomic distances. This approximation is reasonable for most types of interaction; only inherent many-body effects such as polarization may not be adequately described by a pairwise decomposable potential. A potential model for van der Waals type interactions usually consists of a repulsive core with an attractive tail such as the empirical Lennard–Jones potential. Simulation of classical dynamics is straightforward in principle. The forces are calculated from the interaction potential, and Newtonian equations of motion are integrated with an appropriate integrator (see, e.g., [46, 47]). In a mixed quantum/classical molecular dynamics simulation the classical degrees of freedom undergo Newtonian dynamics as in a purely classical simulation. The only difference is in the forces on the classical degrees of freedom, as will be discussed in subsequent sections. In simulations, classical or mixed quantum/classical, there are a few subtleties including the treatment of long-range electrostatic interactions (see, e.g., [48–51]), the treatment of intramolecular interactions, or, alternatively, the constraining of molecular conformations (e.g., [52–54]) and obtaining of properties within the thermodynamic ensemble of interest (e.g., [55–59]).

A large number of properties can be calculated in a molecular dynamics simulation ranging from structural properties to dynamical and spectral properties. When quantum degrees of freedom are involved in principle these properties can be calculated analogously to the classical case, but especially transport properties may suffer from poor convergence. For a discussion and references on this topic, see [44]. Structural information, such as radial distribution functions, structure factors, and coordination numbers, can be obtained. Dynamical information includes diffusion coefficients (see [60–62] for some examples dealing with excess electrons) and other transport properties such as viscosity and thermal conductivity. For mixed quantum/classical systems, spectral properties are also of interest. The density of states, the absorption spectrum, the mean excitation energy (band gap between ground state and first excited state), and the onset of the continuum of excited states can be determined (e.g., [63–66]). More recently pump-and-probe experiments have been simulated [67–71]. These experiments yield time-resolved information on the spectral evolution, the so-called spectral traces. When the time resolution is sufficient this method not only serves to probe the spectral composition of the absorption band, but also provides a means to investigate the coupling between the properties of the quantum subsystem and the dynamics of the classical system.

2. MIXED QUANTUM/CLASSICAL DYNAMICS

2.1. *Separation of Degrees of Freedom: The Ehrenfest Approach*

This section explains commonly used approximations and simplifications for the simulation of a system in which quantum effects of a limited number of degrees of freedom are important. The system is separated in a subsystem of slow degrees of freedom, which will ultimately be treated as classical, and fast degrees of freedom, which will retain their quantum mechanical nature. For example, for a system consisting of many atoms, one might designate (some of) the electrons as the fast degrees of freedom and the nuclei as the slow degrees of freedom. Note that the existence of separation in time scales is crucial when

the classical limit is ultimately taken for the slow degrees of freedom. One has to be very careful in dividing a system into classical and quantum mechanical parts see, e.g., Ref. [72], especially when time scales are comparable.

Note that the notation introduced here—subscripts c and q—anticipates which degrees of freedom are going to be treated classically (c) and which quantum mechanically (q). This notation may be dropped in the remainder of this paper when confusion is unlikely.

Rigorously speaking the quantum nature of all degrees of freedom has to be accounted for, irrespective of the designation "slow" or "fast." The time-dependent Schrödinger equation for the entire system has to be solved. The total wave function $\Psi(\mathbf{r}, \mathbf{R}, t)$ is the solution of

$$i\hbar \frac{\partial \Psi(\mathbf{r}, \mathbf{R}, t)}{\partial t} = H\Psi(\mathbf{r}, \mathbf{R}, t), \tag{1}$$

where H is the Hamiltonian, $\mathbf{r}$ are the coordinates of the fast degrees of freedom, and $\mathbf{R}$ are those of the slow ones. Note that fast coordinates—which are going to be treated quantum mechanically—are labeled with lower case letters while slow coordinates—which are ultimately going to be treated classically—are denoted by capital letters. The vector $\mathbf{R}$ thus is a $3N$-dimensional vector containing the coordinates $\mathbf{R}_j$ of all N slow degrees of freedom in the system; similarly $\mathbf{r}$ is a $3n$-dimensional vector.

The Hamiltonian H of the system of N slow degrees of freedom with mass M and n fast degrees of freedom of mass m is

$$H = K_c + H_q.$$

Here K_c is the kinetic energy operator

$$K_c = -\sum_{I=1}^{N} \frac{\hbar^2}{2M_I} \nabla^2_{\mathbf{R}_I},$$

and the Hamiltonian for the fast subsystem H_q is of the form

$$H_q(\mathbf{r}, \mathbf{R}, t) = -\sum_{i=1}^{n} \frac{\hbar^2}{2m} \nabla^2_{\mathbf{r}_i} + V_{qq}(\mathbf{r}, t) + V_{cc}(\mathbf{R}, t) + V_{qc}(\mathbf{r}, \mathbf{R}, t)$$

when pairwise additive interactions are assumed. The terms in H_q are the kinetic energy operator $K_q = -\sum_{i=1}^{n} (\hbar^2/2m)\nabla^2_{\mathbf{r}_i}$; the potential energy operators for the fast subsystem and the slow subsystem; and the interaction between the two. We group the last three terms as $V(\mathbf{R}, \mathbf{r}, t) = V_{qq} + V_{qc} + V_{cc} = V_q + V_{cc}$.

The Ehrenfest method can be derived as a classical limit of time-dependent self-consistent field method (TDSCF) (see, e.g., [7, 73]). This is a mean field method; i.e., the total wavefunction Ψ of the system is factorized into a single product of that for the slow and fast particles [74],

$$\Psi(\mathbf{R}, \mathbf{r}, t) = \psi(\mathbf{r}, t)\chi(\mathbf{R}, t) e^{\left(i/h \int^t \langle \Psi | H | \Psi \rangle_{\mathbf{R},\mathbf{r}} dt'\right)}, \tag{2}$$

where ψ and χ are supposed to be normalized. The phase factor introduced in this equation is added for simplification of the final equations and the subscript to $\langle\ \rangle$ indicates which degrees of freedom are integrated over. If one substitutes this equation into the time-dependent Schrödinger equation (1) and multiplies from the left with χ^* and integrates over $\mathbf{R}$ one obtains an equation for the wavefunction ψ of the fast degrees of freedom. Similarly,

multiplying by ψ^* and integrating over the fast degrees of freedom yields an equation for χ. These equations are the standard TDSCF equations,

$$i\bar{h}\frac{\partial \psi}{\partial t} = (K_q + \langle \chi | V | \chi \rangle_{\mathbf{R}})\psi \tag{3}$$

and

$$i\bar{h}\frac{\partial \chi}{\partial t} = (K_c + \langle \psi | H_q | \psi \rangle_{\mathbf{r}})\chi. \tag{4}$$

The fast degrees of freedom move on an effective potential energy surface that is an average field of the slow degrees of freedom, and vice versa. Feedback between the fast and slow subsystems is incorporated in an average manner. These two equations have to be solved self-consistently.

In order to obtain the classical limit for the slow degrees of freedom one can follow in the footsteps of Messiah [7] and separate the wavefunction χ for the slow degrees of freedom in amplitude and phase factors.

$$\chi(\mathbf{R}, t) = A(\mathbf{R}, t)e^{(i/\bar{h})S(\mathbf{R},t)}. \tag{5}$$

When one substitutes this into (4) and separates real and imaginary parts (A and S are taken to be real-valued here) one obtains the two equations

$$\frac{\partial S}{\partial t} + \sum_I \frac{\left(\nabla_{\mathbf{R}_I} S\right)^2}{2M_I} + \langle \psi | H_q | \psi \rangle_{\mathbf{r}} = \sum_I \frac{\bar{h}^2}{2M_I}\frac{\nabla^2_{\mathbf{R}_I} A}{A} \tag{6}$$

and

$$\frac{\partial A}{\partial t} + \sum_I \frac{1}{M_I}\left(\nabla_{\mathbf{R}_I} A\right) \cdot \left(\nabla_{\mathbf{R}_I} S\right) + \sum_I \frac{1}{M_I}\frac{A}{2}\nabla^2_{\mathbf{R}_I} S = 0. \tag{7}$$

The latter equation expresses continuity of flux [7]. The classical limit is obtained by setting $\bar{h}$ to zero. Note that $\bar{h}$ does not appear in the latter equation. $\bar{h}$ appears on both sides of (6) but on the left-hand side it appears in $\langle \psi | H_q | \psi \rangle_{\mathbf{r}}$, which is integrated over the quantum degrees of freedom. Hence the classical limit is obtained by setting $\bar{h}$ to zero on the right-hand side of (6), which gives

$$\frac{\partial S}{\partial t} + \sum_I \frac{\left(\nabla_{\mathbf{R}_I} S\right)^2}{2M_I} + \langle \psi | H_q | \psi \rangle_{\mathbf{r}} = 0. \tag{8}$$

This equation, together with (7), describes a swarm of independent classical trajectories moving on the average potential energy surface of the fast particles. The solution S of Eq. (8), which is the Hamilton–Jacobi equation [75], is the classical action $S = \int^t (K_c - V_c)\, dt'$. It can be shown that the Hamilton–Jacobi equation is equivalent to the Newtonian equation of motion [7]

$$\mathbf{F} = -\nabla_{\mathbf{R}} \langle \psi | H_q | \psi \rangle_{\mathbf{r}}, \tag{9}$$

where $\mathbf{F}$ is the force $m(d^2\mathbf{R}/dt^2)$. The separation into a classical and quantum mechanical subsystem is made complete by setting the coordinates $\mathbf{R}$ of the classical system to a δ-function in (3) [76]

$$i\hbar\frac{\partial\psi}{\partial t} = (K_q + V)\psi = H_q\psi. \tag{10}$$

These last two equations define the mixed quantum/classical dynamics within a mean field approximation.

2.2. *The Quantum Force: Hellmann–Feynman Theorem*

The expression for forces on classical particles (Eq. (9)) is commonly rewritten in a more suitable form that does not require the calculation of gradients of wavefunctions. When the quantum wavefunction ψ is an exact solution of (3) the expression in Eq. (9) for forces on classical particles can be simplified to [77]

$$\mathbf{F}_j(\mathbf{R}(t)) = -\left(\left\langle\nabla_{\mathbf{R}_j}\psi|H_q|\psi\right\rangle_{\mathbf{r}} + \left\langle\psi\middle|\nabla_{\mathbf{R}_j}H_q\middle|\psi\right\rangle_{\mathbf{r}} + \left\langle\psi|H_q|\nabla_{\mathbf{R}_j}\psi\right\rangle_{\mathbf{r}}\right) \tag{11}$$

$$= -\left\langle\psi\middle|\nabla_{\mathbf{R}_j}H_q\middle|\psi\right\rangle_{\mathbf{r}} \equiv \mathbf{F}_j^{HF}(\mathbf{R}(t)). \tag{12}$$

Equation (12) is known as the Hellmann–Feynman theorem. It is easy and useful to show that it is true for for the case where ψ is an exact solution of the time-independent Schrödinger equation

$$H_q(\mathbf{r}, \mathbf{R}, t)\psi(\mathbf{r}, \mathbf{R}(t)) = E(\mathbf{R}(t))\psi(\mathbf{r}, \mathbf{R}(t)), \tag{13}$$

where E is the total energy $\langle\psi|H_q|\psi\rangle_{\mathbf{r}}$. Then

$$\left\langle\nabla_{\mathbf{R}_j}\psi|H_q|\psi\right\rangle_{\mathbf{r}} + \left\langle\psi|H_q|\nabla_{\mathbf{R}_j}\psi\right\rangle_{\mathbf{r}} = E\nabla_{\mathbf{R}_j}\langle\psi\mid\psi\rangle_{\mathbf{r}} = 0 \tag{14}$$

when the quantum coordinates are integrated over all space. Note that "exact" in this context means that ψ is an exact solution obtained by using a maybe-not-so-exact Hamiltonian. Sometimes it is not possible to obtain exact solutions to the Schrödinger equation, in which case the Hellmann–Feynman theorem is no longer valid.

2.3. *Adiabatic Approximation*

We have used ψ to denote a general quantum wave function. Assume that at time $t = 0$ the system starts out in a "pure" quantum state, i.e., ψ equals a solution ϕ_k of the time-independent Schrödinger equation at that time

$$H\phi_k = \epsilon_k\phi_k.$$

The solutions of this eigenvalue equation are the energy eigenvalues $\epsilon_k = \epsilon_k(\mathbf{R}(t)) = \langle\phi_k|H_q|\phi_k\rangle_{\mathbf{r}}$ and the adiabatic eigenstates $\phi_k = \phi_k(\mathbf{r}; \mathbf{R}(t))$ for a given configuration $\mathbf{R}$ at time t. So the adiabatic energy surfaces are obtained by solving the time-independent Schrödinger equation and are parameterized by the classical configuration $\mathbf{R}$. At a later time

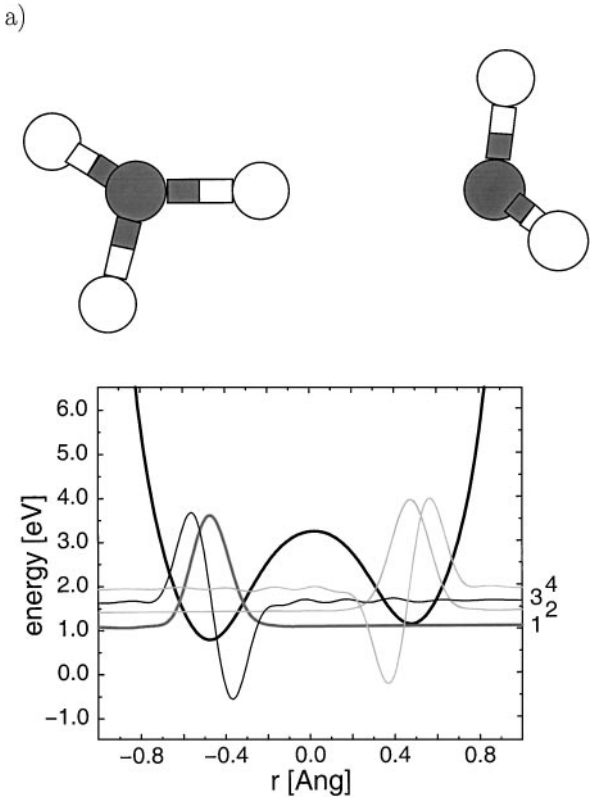

FIG. 1. An example of potential energy surfaces and accompanying wavefunctions for the middle quantum proton in $H_5O_2^+$ in the gas phase. (The quantum proton is depicted at its ground-state expectation value for position.) Top: (a) non-equilibrium and (b) equilibrium configurations (oxygen, black circles; hydrogen, open circles). Bottom: potential surface and wavefunctions for configurations shown. The wavefunctions are labeled according to energy starting with one for the ground state. Note that in the top and bottom figures distances are not scaled the same.

t' the system will generally have developed into an admixture of states

$$\psi(\mathbf{r}, \mathbf{R}, t') = \sum_k c_k(t)\phi_k(\mathbf{r}; \mathbf{R}(t')). \tag{15}$$

We will call this admixture a mixed state. In the adiabatic limit, however, the quantum subsystem is assumed to immediately adapt its state to that of the classical subsystem so that it remains in the initial quantum state (usually the ground state) at all times, i.e., the wavefunction does not become a mixed state and $\psi = \phi_k$ with k fixed. Many simulations have been done within the adiabatic, or Born–Oppenheimer, approximation, where the quantum system is assumed to remain in the ground state [8]. This approximation is valid for systems in which the dynamics is dominated by that of the ground state. In many systems the adiabatic approximation breaks down, however, and excitations from the initial state become important in the time evolution of the system. This is called nonadiabatic dynamics. Departure from adiabaticity becomes likely in regions where the quantum levels are close in energy and in regions of strong coupling between the quantum states. Then proper inclusion

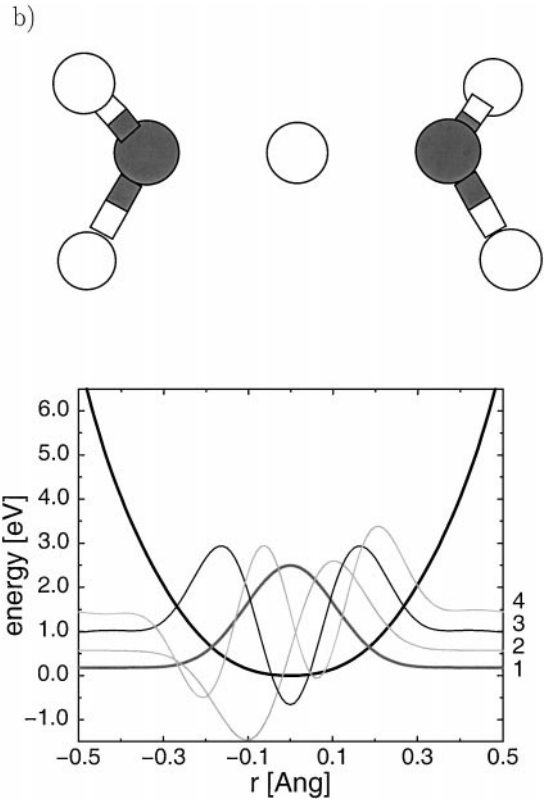

FIG. 1—*Continued*

of nonadiabatic effects is important. Methods for simulation of nonadiabatic events (e.g., [1, 78–82]) will be discussed extensively.

2.4. *Modeling the Interaction between Quantum and Classical Degrees of Freedom: Pseudopotentials*

Simulation of a mixed quantum/classical system within a wavefunction approach requires determination of the eigenstates of the quantum subsystem for a given configuration of the classical system. The interaction between the classical and the quantum subsystem has to be calculated for this purpose. An approximation of both terms V_{qc} and V_{qq} (see Section 2.1), i.e., the pseudopotential, needs to be found. For a general theory on the calculation of pseudopotentials, see, for instance, Austin *et al*. [83].

A pseudopotential has to meet a set of requirements in order to be a sufficiently accurate approximation to the true potential operator for the system. First, the energy conservation of the total system should not be violated. Second, if dealing with an excess electron, the wave function of the excess electron has to be orthogonal to the filled atomic orbitals of the solvent atoms/molecules (Pauli principle). When dealing with an excess quantum proton, usually the overlap of the proton wavefunction with that of the protons in the nucleus can be neglected safely. Third, polarization effects of the atom due to the presence of an excess charge have to be included. Finally, a pseudopotential should reproduce experimentally determined

properties such as scattering cross sections, absorption spectra, etc. In order to meet this last requirement interactions such as exchange effects, Coulombic interactions, and correlation between the motion of the excess electron and the core electrons need to be included. It is possible to construct a pseudopotential that incorporates the requirements exactly, but the resulting pseudopotential is non-local; i.e., the interactions are not pairwise additive and many-body effects have to be taken into account self-consistently. The construction of a local pseudopotential is based on the assumption that the interaction of an excess quantum particle with the classical particles is additive, i.e., that it can be written as a sum of separate interactions with one atom.

An example of potential surfaces for a quantum particle and its wavefunctions is given in Fig. 1. In this gas-phase $H_5O_2^+$ system the middle proton is treated as a one-dimensional quantum particle moving along the oxygen-oxygen axis. Two configurations are shown with accompanying one-dimensional potential surfaces and adiabatic vibrational wavefunctions as a function of the one-dimensional quantum coordinate r along the oxygen–oxygen axis. The potential for the quantum proton depends on the coordinates of all particles in the system. In this figure one sees that the donor–acceptor distance greatly influences the shape of the potential surface. For a larger donor–acceptor distance the potential is a double well, while for a shorter distance it is a single well. The shape of the potential energy surface in turn determines the shape, localization, and energies of the adiabatic eigenstates.

2.5. *Nonadiabatic Dynamics and Branching Processes*

In mixed quantum/classical systems the calculation of the forces is not a trivial issue. Adiabatic simulation methods, in which the quantum subsystem is constrained to occupy the single ith adiabatic eigenstate at all times ($\psi = \phi_i$) are correct when the adiabatic approximation is valid. The expression for the quantum force in this case is given by $-\langle \phi_i | \nabla_{\mathbf{R}} H_q | \phi_i \rangle_{\mathbf{r}}$ (assuming the Hellmann–Feynman theorem is valid) (Section 2.2). When the adiabatic approximation breaks down, however, excited states play a role in the dynamics, and propagation in time of an initially pure quantum wave function generally evolves the wavefunction to a mixed state. The simplest way to include excited states is to let the system evolve naturally into a mixed state and use a mixed state $\psi = \sum_i c_i \phi_i$ in the energy and force calculation. If one treats the entire system quantum mechanically this is not a problem. The dynamics of the total quantum mechanical system is correctly described by mixed states. When the classical limit is taken in the mean field approach (Section 2.1), however, the different treatment of classical and quantum degrees of freedom does not always result in a correct description of the overall dynamics. The expansion of the total wavefunction Ψ into a single product (configuration) neglects the correlation between the different types of degrees of freedom. We illustrate this with an example.

Consider, e.g., a system that consists of a polar solvent in which a large solute complex that has an ionic and a covalent state is immersed, as illustrated in Fig. 2. The ionic and covalent states of this system are of different character and the orientation of the solvent molecules around the solute is entirely different dependent on the state of the solute. The charge separation within the solute complex in the ionic state orders the dipole moments of the solvent molecules around the solute, while for the covalent state the solvent molecules are oriented in a more random fashion. Assume that for this solvent–solute system the only degree of freedom that needs to be treated quantum mechanically is the charge transferring between covalent and ionic state (a hydride in this example). Using a mean field method

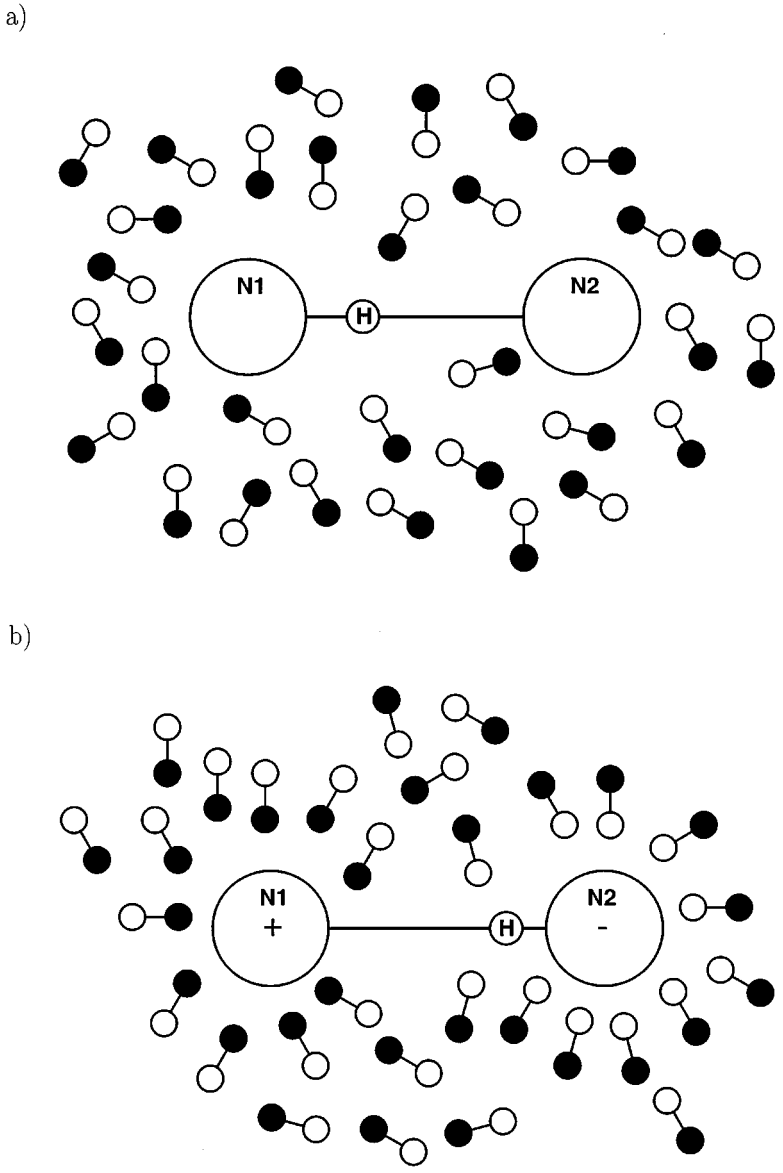

FIG. 2. A complex immersed in a polar solvent; the solvent molecules consist of a positively charged part (white) and a negatively charged part (black). When the complex is in a covalent state (a) the solvent molecules are oriented rather randomly about the complex; in the ionic state (b), however, there is a distinct favorable orientation around the solute for the solvent molecules. The charge distribution in the solute complex is pictured on parts of the complex for clarity. Only the solvent molecules closest to the complex are shown.

the forces on the classical solvent are averaged over both ionic and covalent state wavefunctions at all times $t > 0$. This means that the forces are a weighted average of the forces corresponding to the ionic state and the forces corresponding to the covalent state (where the squares of the amplitudes c_i are the weights). This is a reasonably good description of the situation when the dynamics of the system is dominated by one state, provided that one is interested in properties of that dominant state. Little information, however, concerning properties of the other non-dominant state can be obtained using a mean field method. Also,

when both states of the system are important in the dynamics, an average treatment does not reproduce the actual dynamics correctly.

When the classical dynamics depends strongly on the quantum path and multiple distinct paths from an initial to a final state are possible in the dynamics we speak of a branching process. A mean field method is not expected to work very well for describing branching processes and one has to use a different approach. This approach is based on nonadiabatic events, where departure form adiabaticity is modeled by state switches of the quantum subsystem between different quantum states. This is called surface hopping. As in the other methods the quantum and classical parts of the system have to be treated self-consistently. The trajectories of the classical particles determine the probabilities for quantum transitions and the quantum transitions, in turn, influence the classical trajectories. We focus on these nonadiabatic methods in the remainder of this paper.

2.6. *Separation of Degrees of Freedom: A Multi-configurational Approach*

The separation of the degrees of freedom in a fast and slow subsystem in the surface hopping approach is achieved by a route analogous to the Ehrenfest approach discussed in Section 2.1 (for notation one is referred to that section) [74, 76, 84]. Instead of approximating the total wavefunction Ψ as a single product as in the Ehrenfest approach, a multi-configurational expansion is used that includes the correlation between the different degrees of freedom

$$\Psi(\mathbf{r}, \mathbf{R}, t) = \sum_k \chi_k(\mathbf{R}, t)\phi_k(\mathbf{r}; \mathbf{R}). \tag{16}$$

The fast particle basis functions ϕ_k are assumed to be orthonormal and to be specified in advance (hence the switch in notation from ψ to ϕ), i.e., that an adiabatic or diabatic basis is used. Adiabatic surfaces are instantaneous solutions of the time-independent Schrödinger equation. In principle they are linear combinations of diabatic surfaces. (For a review on the use of a diabatic versus adiabatic basis see, e.g., Refs. [85, 86].) The slow particle wavefunction need not be normalized. Substitution of this expression into the time-dependent Schrödinger equation and some manipulations yield a coupled set of equations for the slow degrees of freedom and for the fast degrees of freedom, analogous to the expressions obtained in the Ehrenfest approach. The slow degrees of freedom obey

$$i\bar{h}\frac{\partial \chi_k(\mathbf{R}, t)}{\partial t} = K_c\chi_k(\mathbf{R}, t) + \sum_{k' \neq k}(E_{kk'} - D_{kk'})\chi_{k'}(\mathbf{R}, t), \tag{17}$$

where $E_{kk'} = \langle\phi_k|H_q|\phi_{k'}\rangle_{\mathbf{r}}$ and and $D_{kk'}$ is the nonadiabatic operator

$$D_{kk'}(\mathbf{R}, t) = -\sum_{I=1}^{N}\left(\frac{\bar{h}^2}{2M_I}\langle\phi_k|\nabla^2_{\mathbf{R}_I}|\phi_{k'}\rangle_{\mathbf{r}} + \frac{\bar{h}^2}{M_I}\langle\phi_k|\nabla_{\mathbf{R}_I}|\phi_{k'}\rangle_{\mathbf{r}}\nabla_{\mathbf{R}_I}\right). \tag{18}$$

Surface hopping is a classical analog of this expression, not an exact classical limit. As explained nicely in a recent publication by Tully [76] the wavefunctions χ_k of the slow degrees of freedom can be separated again in amplitude, A, and phase, S, factors. After we

obtain the classical limit by setting $\hbar$ to zero, the equation

$$\frac{\partial S_k}{\partial t} + \sum_I \frac{\left(\nabla_{\mathbf{R}_I} S_k\right)^2}{2M_I} + \langle \phi_k | H_q | \phi_k \rangle_{\mathbf{r}} = 0 \tag{19}$$

and the flux continuity equation

$$\begin{aligned} &\frac{\partial A_k}{\partial t} + \sum_I \frac{1}{M_I} \left(\nabla_{\mathbf{R}_I} A_k\right) \cdot \left(\nabla_{\mathbf{R}_I} S_k\right) + \sum_I \frac{1}{M_I} \frac{A_k}{2} \nabla^2_{\mathbf{R}_I} S_k \\ &\quad = -\sum_{k' \neq k} A_{k'} \left(\left[\sum_I \frac{d\mathbf{R}_I}{dt} \cdot \mathbf{d}_{kk'}(\mathbf{R_I}) + \frac{i}{\hbar} E_{kk'} \right] e^{-(i/\hbar)\int^t (E_{k'k'} - E_{kk})\, dt'} \right) \end{aligned} \tag{20}$$

emerge. Here $\mathbf{d}_{kk'}$ is the nonadiabatic coupling vector

$$\mathbf{d}_{kk'}(\mathbf{R}) = \langle \phi_k \mid \nabla_{\mathbf{R}} \phi'_k \rangle_{\mathbf{r}}.$$

For the fast degrees of freedom the equation of motion is again given by (10). Equations (19) and (20) describe motion of trajectories on each effective potential energy surface

$$E_{kk} = \langle \phi_k | H_q | \phi_k \rangle_{\mathbf{r}}, \tag{21}$$

where the flux between the surfaces is governed by the terms containing the off-diagonal elements $E_{kk'}$ or the nonadiabatic coupling vector $\mathbf{d}_{kk'}$ in (20). A practical exact solution to these equations has not been obtained. The fact that trajectories are coupled in a non-local manner hampers a direct solution of these equations. In surface hopping each trajectory evolves independently of the others. This obviously is an approximation. In the next section it will be shown that the expression for the flux between surfaces in surface hopping is essentially equal to the right-hand side of (20) when one identifies A_k with the quantum amplitude on each surface k.

2.7. *Molecular Dynamics with Quantum Transitions: History and Algorithm*

The development of methods to deal with nonadiabatic effects in molecular dynamics has a long history (see, e.g., [87]), in which a variety of classical, semiclassical, and quantum mechanical approaches play a role. The most widely applied method is surface hopping, with its many variants in which a state transition of the quantum particle is described by a "jump" between the potential energy surfaces corresponding to the quantum states. In 1990 Tully proposed a new surface hopping approach, molecular dynamics with electronic transitions (MDET) [1]. This method was originally developed for electronic transitions but more recently has been applied to single proton transfer reactions [88] and been rechristened molecular dynamics with quantum transitions (MDQT). The surface hopping method MDQT allows quantum transitions at any time instead of at localized avoided crossings only, as in the older methods [89]. Moreover, it allows transitions between any number of coupled states maintaining quantum coherence between different "state switches." A swarm of classical trajectories is considered over the effective energy surfaces (20). The system is allowed to make stochastic "hops" between the instantaneous quantum states depending on the time evolution of the occupation probabilities of the states. At a given

time t each trajectory is at a single potential energy surface, never on an average surface, and the wavefunction that determines the forces on the classical particles is never a mixed state. This is a simple solution to the problems that arise when a mixed-state wavefunction is used. For the sake of simplicity, the switches between quantum states are assumed to be sudden and to occur in infinitesimal time. It has to be pointed out, however, that in spite of sudden state switches of a single trajectory, the ensemble of trajectories evolves smoothly because the trajectories switch at different times. At each integration time step a decision of whether to switch states according to a "fewest switches" algorithm governed by the quantum mechanical probabilities is made. The switching procedure in MDQT ensures that, for a large ensemble of trajectories and ignoring difficulties with classically forbidden states, the fraction of trajectories assigned to any state at any time is equal to the average quantum probability at that time.

Here we discuss MDQT in more detail (the equations can be found in many papers, including Ref. [1]) and give some practical points for simulation and other points of interest. Since surface hopping is best suited to the use of an adiabatic basis [76, 77] we represent the formulation in terms of adiabatic eigenstates. The equations that are given are general, however. The time-dependent quantum wavefunction $\psi(\mathbf{r}, \mathbf{R}, t)$ is expanded in a basis of adiabatic eigenstates $\phi_j(\mathbf{r}; \mathbf{R}(t))$ that have energy eigenvalues $\epsilon_j(t) = E_{jj}(t) = \langle \phi_j | H_q | \phi_j \rangle_{\mathbf{r}}$ and depend parametrically on the classical trajectory $\mathbf{R}(t)$;

$$\psi(\mathbf{r}, \mathbf{R}, t) = \sum_j c_j(t) \phi_j(\mathbf{r}; \mathbf{R}(t)), \tag{22}$$

where $c_j(t)$ are the (complex-valued) expansion coefficients, the quantum amplitudes. Substitution of this equation into the time-dependent Schrödinger equation yields the equations of motion (eom) for the expansion coefficients

$$\dot{c}_j \equiv \frac{dc_j}{dt} = -\sum_k c_k \left(\mathbf{d}_{jk} \cdot \dot{\mathbf{R}} + \frac{i}{\hbar} \langle \phi_j | H_q | \phi_k \rangle \right), \tag{23}$$

where $\mathbf{d}_{jk}$ is the previously introduced nonadiabatic coupling vector

$$\mathbf{d}_{jk}(\mathbf{R}) = \langle \phi_j(\mathbf{r}; \mathbf{R}) | \nabla_{\mathbf{R}} | \phi_k(\mathbf{r}; \mathbf{R}) \rangle.$$

Note that the subscript is dropped from $\langle\ \rangle$; the brackets stand for integration over the quantum degrees of freedom only. Comparison of this equation to (20) shows the analogy between the amplitude A_j and the quantum amplitude c_j (apart from the phase factor, which is arbitrary). The diagonal terms $\mathbf{d}_{jk}$ are zero for orthogonal wave functions. In the above derivation of the eom, the chain rule

$$\left\langle \phi_j \left| \frac{\partial \phi_k}{\partial t} \right. \right\rangle = \langle \phi_j | \nabla_{\mathbf{R}} \phi_k \rangle \cdot \dot{\mathbf{R}} \tag{24}$$

was used. In simulations, however, the left-hand side of this equation is computed instead of the right-hand side whenever possible in order to avoid the expensive gradient calculation. In the adiabatic representation the $\langle \phi_j | H_q | \phi_k \rangle$-term in Eq. (23) is equal to $\epsilon_k(\mathbf{R}) \delta_{jk}$. In a diabatic representation the nonadiabatic coupling vectors $\mathbf{d}_{jk}$ are zero [85, 86]. Note that

the second derivative terms present in the nonadiabatic coupling in Eq. (18) are rigorously absent here due to the fact that the coefficients c_j depend on time only and not on the classical coordinates $\mathbf{R}$ as did the expansion coefficients χ_j.

Although the total wave function ψ is a mixed state, in surface hopping the forces on the classical subsystem are determined by a single adiabatic eigenstate, the occupied state. The heart of the MDQT method is the methodology to decide which state is occupied at which time. The diagonal elements of the time-dependent density matrix with elements $a_{kj}(t) = c_k^*(t)c_j(t)$ give the occupation probabilities of the instantaneous adiabatic eigenstates. Thus the number of trajectories—out of a swarm of N trajectories—on potential energy surface j at time t is $a_{jj}(t)N$. The off-diagonal elements give the phase coherence. The probability that a trajectory in state j at time t switches out of this state during the time step δt should be chosen in such a way that an ensemble of trajectories has the correct statistical distribution of occupied states and transition probabilities at all times. Tully proposed the hopping probability

$$g_{jk}(t, \delta t) = \max\left(0, \frac{b_{kj}\delta t}{a_{jj}(t)}\right), \tag{25}$$

where

$$b_{kj} = 2\,\mathrm{Im}\left(\frac{a_{kj}}{\hbar}\langle\phi_k|H_q|\phi_j\rangle\right) - 2\,\mathrm{Re}(a_{kj}\mathbf{d}_{kj}\cdot\dot{\mathbf{R}}), \tag{26}$$

subject to the constraint that the fewest possible switches occur. The coefficients b_{kj} are related to the probability flux by $\dot{a}_{jj} = \sum_{k\neq j} b_{jk}$ (from Eq. (23)). The total change in occupation probability of a given state j contains contributions b_{jk} from all other states involved. When state j is occupied at a given time, a transition to another given state k may occur when the probability flow is from j to k, i.e, $b_{jk} < 0$ (which implies $b_{kj} > 0$ and hence $g_{jk} > 0$). When $b_{jk} > 0$ the hopping probability from state j to state k is set to zero. The transition probabilities are compared to a uniform random number $\zeta \in [0, 1]$ to decide which state the system will jump to in the next time step. Assume that state j is occupied (and this state is neither the ground state nor the first excited state). Then the system will hop to the ground state (labeled 1) if $\zeta \leq g_{j1}$; a switch to the first excited state will occur if $g_{j1} < \zeta \leq g_{j1} + g_{j2}$, etc. This procedure ensures that for an ensemble of trajectories and for infinitesimal δt, the rate of change of number of trajectories in a given state j equals $\dot{a}_{jj}\delta t$, as required: The probability flux from one state to another is correct. For an ensemble of trajectories, the fraction of trajectories at a given time in a certain state is equal to the average occupation probability of that state at that time for all times. This is only true, however, in absence of problems due to classically forbidden states (we will return to this later in this section). Also, for complicated systems of practical interest averaging over an ensemble of trajectories may be computationally very expensive, if not impossible [90–92].

The probability of hopping approaches zero as the time step δt is reduced. Even though each individual trajectory changes when one changes the time step (because they will switch at different times, resulting in completely different dynamics of the individual trajectories) the results for an ensemble of trajectories are independent of the time step as long as the time step is chosen sufficiently small. The MDQT method is summarized in Fig. 3.

In general energy is not conserved when the system jumps from one potential energy surface to another. To correct this, a velocity adjustment should be made. The adjustment

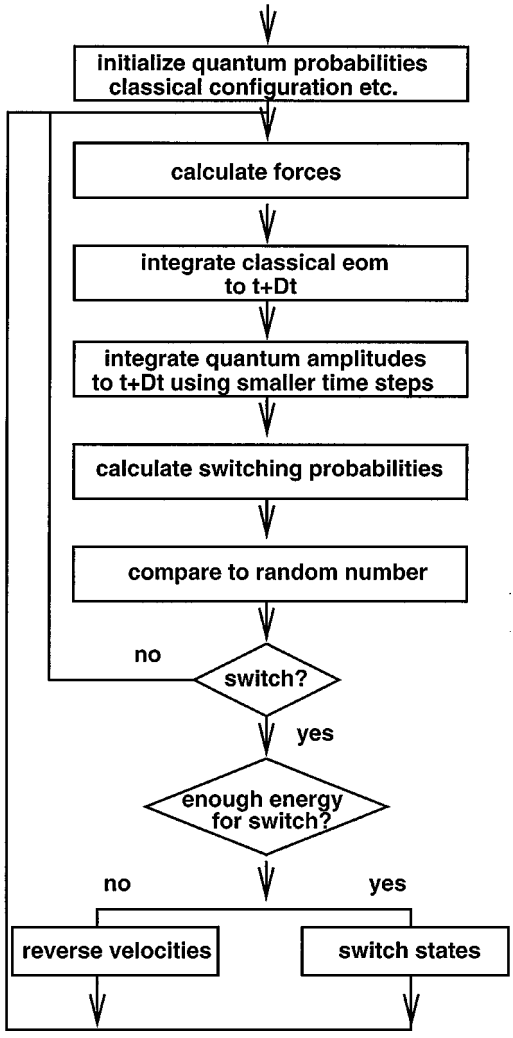

FIG. 3. Overview of MDQT. (Note that the velocity reversal conforms with the original MDQT.)

is usually made in the direction of the nonadiabatic coupling vector, but other approaches are known [93]. The nonadiabatic coupling vector couples with the velocity of the classical particles as $\dot{\mathbf{R}} \cdot \mathbf{d}_{jk}$ so only the component of the velocity parallel to the nonadiabatic coupling vector is adjusted when a trajectory jumps to another state. This means that at those instants the nonadiabatic coupling vector has to be calculated explicitly. The coupling vector can be calculated from the off-diagonal Hellmann–Feynman forces:

$$\mathbf{d}_{jk}(\mathbf{R}) = \frac{\langle \phi_j | \nabla_{\mathbf{R}} H_q | \phi_k \rangle}{\epsilon_k - \epsilon_j}, \qquad j \neq k \tag{27}$$

(This expression can be derived from the fact that $\nabla_{\mathbf{R}} \langle \phi_j | H_q | \phi_k \rangle = 0$ for exact eigenfunctions ϕ.) Note that $\mathbf{d}_{jk} = -\mathbf{d}_{kj}^*$ and the diagonal elements $\mathbf{d}_{kk}$ are zero for orthogonal wave functions; also note that if one imposes bond constraints on atoms within a molecule, the nonadiabatic coupling vector has to satisfy these constraint forces [88]. If there

is not enough energy available in the velocity component parallel to the coupling vector, the intended hop should be rejected. According to the quantum subsystem it is time to switch states, but the classical subsystem cannot provide enough energy for that: It is classically forbidden. These failed hops may occur occasionally simply because of an "unlucky" draw of a random number, but for some systems and for low energies the fraction of rejected hops may be substantial. This is a warning sign of possible breakdown of the mixed quantum/classical description. The branching ratios of the trajectories then no longer equal the average of the squared quantum amplitudes. There are two views on how to handle rejected hops (assuming that a mixed quantum/classical description is valid). The first view is that velocity in the direction of the nonadiabatic coupling vector should be reversed [88]. The physical picture behind this reasoning is that the system tries to hop to an upper surface, cannot make it, and falls back. In the limit of infinitesimal time step $\delta t \to 0$ this is equivalent to the way it is dealt with in methods that use the so-called Pechukas force in the time propagation (Section 2.9.1). The second view is to continue the trajectory as if nothing happened [80]. The idea is that for some systems keeping the same velocities after a rejected state switch results in an error in the occupation probabilities that is less severe than the violation of momentum conservation that would occur when the velocities were reversed. In MDQT momentum generally is not conserved when nonadiabatic transitions occur, but under normal conditions the violation is considered to be minor. In our experience the violation of momentum conservation after velocity reversal is of the same order as the violation that occurs for a successful hop.

The quantum amplitude coefficients can be rapidly oscillating in time, which can easily be seen when one substitutes [84]

$$\psi(\mathbf{r}, \mathbf{R}, t) = \sum_j \tilde{c}_j \phi_j(\mathbf{r}, \mathbf{R}) e^{+(i/\hbar)\int_0^t dt' \epsilon_j(\mathbf{R}(t'))} \tag{28}$$

into the time-dependent Schrödinger equation to obtain

$$\dot{\tilde{c}}_j = -\sum_k \tilde{c}_k \left(\left[\mathbf{d}_{jk} \cdot \dot{\mathbf{R}} + \frac{i}{\hbar} \langle \phi_j | H_q | \phi_k \rangle \right] e^{-(i/\hbar)\int_0^t dt' [\epsilon_k(\mathbf{R}(t')) - \epsilon_j(\mathbf{R}(t'))]} \right) \tag{29}$$

(which shows the analogy to (20) including the phase factor). If the energy gap $\epsilon_j - \epsilon_k$ is large, the phase factor is a rapidly oscillating function in time and the time average of $\dot{\tilde{c}}_j = 0$. Only when the energy gap is relatively small or the states are very strongly coupled will amplitude be redistributed among the different $\tilde{c}_j$'s. Leaking of occupation probability from one state to another only takes place when their energy levels are close for a reasonable amount of time. To avoid problems in integrating the oscillatory coefficients c one can integrate the expression for the $\tilde{c}$'s or a similar expression [88] instead.

In MDQT an independent trajectory approximation is made to the non-locally interacting trajectories obtained by a multi-configurational treatment (Eqs. (19) and (20)). There is no interaction between different trajectories in MDQT; each trajectory is completely independent from the other trajectories in the ensemble. Within one trajectory, however, the equations of motion for the expansion coefficients (Eq. (23) or alternatives such as (28)) are integrated coherently throughout; i.e., the phase factors are retained at all times. This means that within one trajectory there are interference effects of the quantum amplitudes (the expansion coefficients $c_j(t)$) and when a trajectory passes through subsequent regions

of strong coupling there will be interference in the excitation probabilities (Stückelberg oscillations [94]).

2.8. *Mean Field versus Surface Hopping: An Illustration*

In order to summarize and clarify the ideas introduced here Fig. 4 shows possible paths in a two-state model for a mean field method, a naive surface hopping algorithm

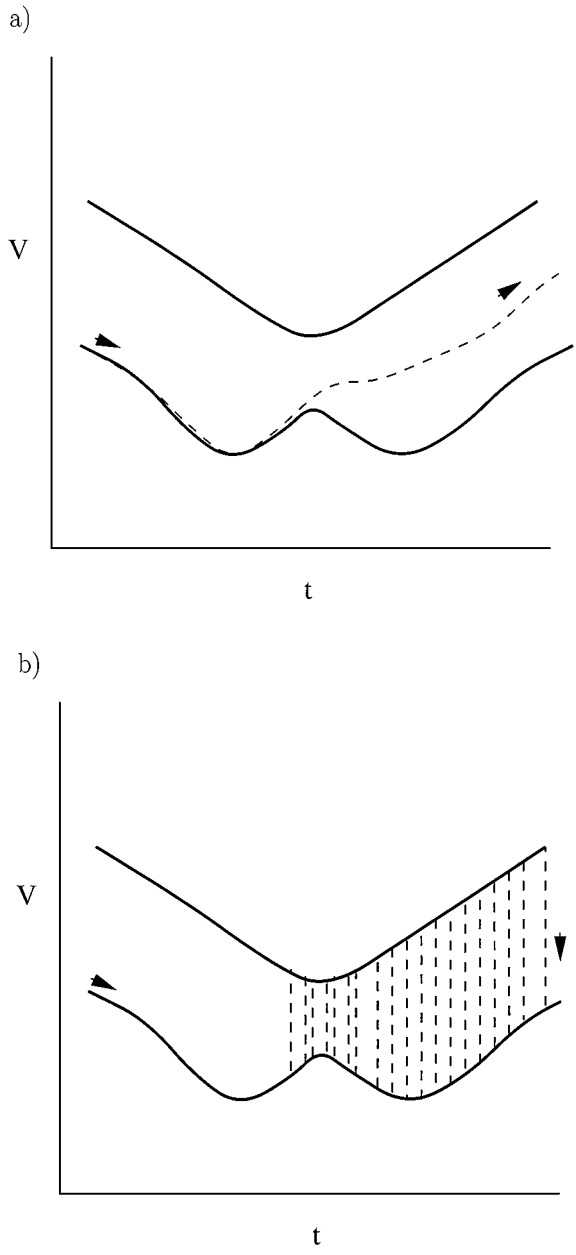

FIG. 4. Upper and lower adiabatic energy curves as a function of time (solid lines) and the potential energy of a possible trajectory (dashed line) for (a) mean field method, (b) naive surface hopping, and (c) MDQT. The arrows indicate the direction of the path.

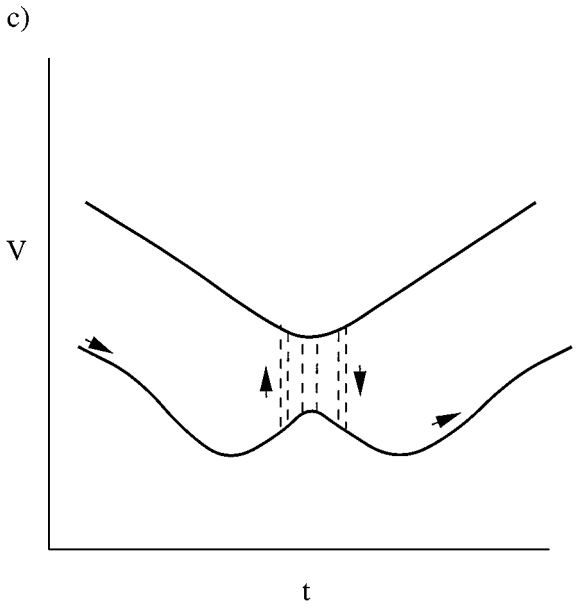

FIG. 4—*Continued*

(where the switching probability depends on instantaneous occupation probability only), and MDQT. The difference between the first method and the latter two lies in the evaluation of the forces on the classical particles, while the difference between the latter two lies exclusively in the hopping criterion. In Fig. 4 two adiabatic energy curves are given as a function of time, i.e., the potential energy surfaces for (classical) nuclear motion if either of these states is occupied. In these graphs the energy of a trajectory—or, in other words, the potential energy surface on which the nuclei move—is depicted as a dashed line. Note that due to time propagation under different forces in each method, the adiabatic energy curves diverge on a longer time scale than depicted here. In Fig. 4a, a trajectory obtained by the mean field method is shown. With the mean field method, the trajectory moves on a single adiabatic surface until the region of strong coupling is reached (where the surfaces are close in energy). After the trajectory leaves this region, the nuclear motion evolves on a potential energy surface that is a weighted average of both adiabats. This method cannot correctly describe branching processes, as shown earlier. Figure 4b depicts a trajectory obtained by a naive surface hopping method. This method behaves similarly to the mean field method: Until the region of strong coupling is reached the system is on a single adiabatic surface, but after leaving the region of strong coupling the system keeps switching states incessantly. This effectively results in movement of the classical nuclei on the same average potential energy surface as obtained by a mean field treatment, which is undesirable in many applications. The numerous state switches occur because this method does not incorporate a fewest switches criterion. If at a given time the flux in occupation probability from a state i to another state j is positive then more trajectories switch from from i to j than from j to i. This results in the correct overall flux of trajectories from state i to state j, but the flux flow is not obtained in the most "straightforward" manner. With a fewest switches criterion only switches from i to j occur. The importance of the fewest switches criterion is underlined by the trajectory obtained with MDQT, as

shown in Fig. 4c. The trajectory moves on a single adiabatic potential energy surface at all times, and only in the region of strong coupling do a few hops occur between the surfaces. In the region of strong coupling motion on an effective surface is correct; MDQT relies on the fact that the time spent in these strong coupling regions is short. Clearly, the fewest switches criterion in MDQT is essential for a proper description of branching processes.

As pointed out previously, however, there are situations for which a mean field treatment is the method of choice. In situations were the mean field method works, it has the advantage that it has a well-defined classical limit, is independent of representation (i.e., whether a diabatic or adiabatic basis is used [85, 86]), conserves total energy naturally, and includes feedback between the classical and quantum subsystem, which is not the case in some mixed quantum/classical methods. In some cases a mean field approach is shown to outperform surface hopping [95] and in some instances surface hopping is shown to perform rather poorly [96]. Especially for cases where the regions of strong nonadiabatic coupling are extended, surface hopping has some problems. It is the mixed quantum/classical method of choice, however, for the applications we consider in this paper.

2.9. *Alternatives to Molecular Dynamics with Quantum Transitions*

2.9.1. The Pechukas force. In search of an appropriate way to mix quantum and classical mechanics, Pechukas [97, 98] developed a semiclassical theory for time propagation of a mixed quantum/classical system. The separation of degrees of freedom is based on the same principles as discussed in Sections 2.1 and 2.6. Pechukas' work is based on a generalization of Hamilton's formalism and Feynman's path-integral formulation of quantum mechanics [10]. He formulated a semiclassical theory of potential scattering and derived "classical" equations for the relative motion of two colliding atoms when they undergo an internal quantum transition. The expression for the force in this formalism has been used in mixed quantum/classical simulations of various systems.

The Hamiltonian H is split into a nuclear kinetic energy part, K_c, and everything else, $H_q(\mathbf{r}, \mathbf{R})$. As usual, $\mathbf{R}$ are the coordinates of the nuclei (that will ultimately be treated classically), and $\mathbf{r}$ specifies the internal states of the atoms, for example, electronic, rotational, or vibrational states. Propagation of the system from $\{\mathbf{r}'\mathbf{R}'t'\}$ to $\{\mathbf{r}''\mathbf{R}''t''\}$ under this Hamiltonian is described by the full propagator $K(\mathbf{r}''\mathbf{R}''t'' \mid \mathbf{r}'\mathbf{R}'t')$. For calculation of the mixed quantum–nuclear dynamics computation of the full propagator is not necessary, however. Instead, it is sufficient to calculate a reduced propagator $K_{\beta\alpha}$, where $K_{\beta\alpha}$ gives the probability of an internal transition $\alpha \to \beta$ while the atoms move from the space-time point $\{\mathbf{R}'t'\}$ to $\{\mathbf{R}''t''\}$. This reduced propagator can be evaluated in the Feynman path-integral notation and the full time propagation is divided into P time slices of $\epsilon = (t'' - t')/P$. The path-integral expression can be approximated by a short-time expression for sufficiently small time slices, i.e., large P (ideally $P \to \infty$). This allows factorization of the propagator into a potential and a kinetic energy part as a reasonable approximation to the full propagator. This considerably simplifies the expression to be evaluated.

In the classical limit, $\hbar \to 0$, only the immediate neighbors of stationary phase points contribute to the path integral. In the semiclassical approximation it is assumed that the magnitude of the transition amplitude of state α to state β changes much more slowly with variations in the path than its phase. Stationary phase paths contribute most significantly to the reduced propagator $K_{\beta\alpha}$. The reduced propagator $K_{\beta\alpha}$ combined with the stationary

phase requirement leads to the classical equation of motion

$$M\ddot{\mathbf{R}}(t) = -\mathrm{Re}\left\{ \frac{\langle \beta(t,t'')|\partial H_q(\mathbf{r},\mathbf{R}(t))/\partial \mathbf{R}(t)|\alpha(t,t')\rangle}{\langle \beta(t,t'') \mid \alpha(t,t')\rangle} \right\} \equiv \mathbf{F}^P(\mathbf{R}(t)), \qquad (30)$$

where $\mathbf{R}(t)$ is a stationary phase path. The above equation is the well-known Newtonian equation of motion $M\mathbf{a} = \mathbf{F}$ in disguise, where the force is the Pechukas force $\mathbf{F}^P$. This expression is much more complicated than that for the Hellmann–Feynman force (Eq. (12)). The wavefunctions $\alpha(t,t')$ and $\beta((t,t'')$ are dynamical wavefunctions. Relating to our previous notation, $\alpha(t,t') \equiv \psi_\alpha(t)$, where $\psi_\alpha(t)$ is obtained by propagating adiabatic state $\alpha \equiv \phi_\alpha$ in time from t' to t. The dynamical wavefunctions are a solution of the time-dependent Schrödinger equation and are generally a mixed state obtained by time propagation under the time-dependent Schrödinger equation with time-dependent Hamiltonian $H_q(t)$. The denominator of the expression for the Pechukas force $\langle \beta(t,t'') \mid \alpha(t,t')\rangle$ is the transition amplitude $T_{\beta\alpha}$ from state α to state β. $T_{\beta\alpha}$ is time reversible and is best understood as the overlap of the dynamical mixed state wavefunction $\alpha(t'',t') \equiv \psi_\alpha(t'')$ with the adiabatic eigenstate β at time t'' (or equivalently of the back-propagated state $\beta(t',t'')$ with state α at time t').

The Pechukas force describes a semiclassical path for the classical subsystem when the quantal subsystem evolves from state α to state β. An important point to note is that the Pechukas force is not predictive. The force along a trajectory depends on the entire trajectory itself. Hence, the forces and the trajectories need to be solved self-consistently. The computational effort to achieve self-consistency depends on the physical problem at hand and cannot be accomplished for large-scale simulations. This is one of the problems of the method and is associated with the bifurcation of classical paths (Section 2.5). In practice this limits the self-consistent propagation to short times. Also note that the expression for the Pechukas force intrinsically includes a finite time interval. Pechukas showed that the energy and angular momentum are rigorously conserved along a trajectory. The differences in energy associated with a quantum transition are balanced by a change in energy of the classical subsystem. The same holds for the angular momentum.

2.9.2. Nonadiabatic methods based on non-Hellmann–Feynman forces. Webster, Rossky, and Friesner developed a nonadiabatic simulation method (the WRF method for short) [78] that combines the Pechukas approach with a surface hopping method. The Pechukas force determines the best classical trajectory accompanying the quantum evolution from a given initial state to a given final state. The self-consistent propagation associated with the use of the Pechukas force is limited to short times for mixed quantum/classical simulations (see Section 2.5) and to overcome the problems associated with long-time mixed state propagation the quantum subsystem is projected onto an adiabatic eigenstate at intervals. An initial state of the system $\psi_\alpha(t_i) = \alpha$ is selected at t_i from the set of adiabatic eigenstates $\{\alpha_i(t_i)\}$ and the time-dependent Schrödinger equation is solved. The state of the system $\psi_\alpha(t)$ at a later time t_f will have developed an admixture of adiabatic states and the overlap of this wavefunction with the adiabatic eigenstate $\beta \in \{\beta_i(t_f)\}$ at this time gives the transition amplitude $T_{\beta\alpha} = \langle \beta \mid \psi_\alpha(t_f)\rangle$. An analog to the stochastic surface hopping method MDQT [1] is used to determine into which instantaneous eigenstate the system should be projected at a given time. The squares of the transition amplitudes $T_{\beta\alpha}$, instead of the $g_{\alpha\beta}$ as in MDQT, define the probability of transition to each adiabatic state. The decision of which adiabatic eigenstate will be occupied at a given classical time step is made on the first iteration through the self-consistent calculation of the path and the force along the path.

Theoretically, energy is rigorously conserved in this method, without any need for velocity rescaling. In practice, energy conservation may be hard to obtain.

A comparison has been made between the WRF method and MDQT by the authors of the former method [99]. This comparison was made for two-state systems that do not explicitly incorporate bath dynamics but include an arbitrary dephasing time scale. The results do not seem to strongly favor use of the one method over the other. No conclusion about which is the "better" method can be drawn. Note that the WRF method and MDQT give the same results in two limits: In the limit of infinitesimal time step the effect of the Pechukas force is equivalent to the velocity rescaling used in MDQT when a state transition occurs. In the adiabatic limit the Pechukas force reduces to the Hellmann–Feynman expression.

A hybrid method has been developed that combines the use of the Pechukas force with Tully's surface hopping method [80]. The transition probabilities $g_{\alpha\beta}$ (rather than $T_{\alpha\beta}$ as in WRF) are obtained by back-propagation of the wave functions. Analogous to the original WRF method, this method selects an instantaneous adiabatic eigenstate after each classical time step that determines the quantum forces. For details the reader is referred to the article of Coker *et al*. [80] or to the review article by the same author [84], where all the above issues are discussed.

Recently another mixed quantum/classical formalism for nonadiabatic QMD was presented by Murphrey and Rossky [100]. Their method was developed for quantal subsystems represented by approximate wavefunctions. It is based on a stationary-phase approximation of the classical bath and a variational principle for the quantum transition amplitudes. The approximate trial wavefunctions differ only by a first order variation from the exact solutions of the time-dependent Schrödinger equation and are assumed to give the stationary value for the transition amplitudes [101]. A variational expression for the transition amplitudes is derived that is stationary with respect to small changes in the trial wavefunctions. Thus first order errors in the trial wavefunctions result in second order errors in the transition amplitudes. The expression for the quantum force is slightly more complicated than in the WRF approach. It contains the gradient not only of the Hamiltonian H_q but also of the trial wavefunctions $\breve{\alpha}$ and $\breve{\beta}$. (The appearnace of gradients of the wavefunctions in this expression is expected because we are dealing with approximate wavefunctions (see Section 2.2).) The expression for the "generalized stationary phase" quantum force is

$$\mathbf{F}^G(\mathbf{R}(t)) = -\mathrm{Re}\left\{ \frac{\nabla_{\mathbf{R}} \langle \breve{\beta}(t, t_f) | H_q(\mathbf{r}, \mathbf{R}(t)) | \breve{\alpha}(t, t_i) \rangle}{T_{\beta\alpha}} \right\}, \tag{31}$$

where $T_{\beta\alpha}$ is given by the same expression as in WRF. The force and trajectory calculations have to be done self-consistently in the same manner as in WRF, and the energy is conserved independent of the energy difference between initial and final states. This method suffers from the same problems regarding long-time evolution as the WRF approach, and surface hopping is used to limit mixed state propagation to short times.

Although so far this algorithm has only been applied to a simple test problem, the results seem promising. The authors find that the results converge faster with increasing basis set size (for the expansion of the eigenstates) than when the Hellmann–Feynman force is used. Moreover, they find that for a limited basis set their results are much closer to the exact ones. Compared to simulations based on the Pechukas force they find that this algorithm is more robust with respect to the time step and only slightly more expensive computationally speaking. The appearance of the gradients of the approximate wavefunctions in the expression

for the force, however, could make this algorithm less tractable for other systems than those considered by these authors. The effort to calculate the gradients depends greatly on the choice of the basis functions for the trial wavefunctions and may be substantial or even close to prohibitive (see Section 4).

The major disadvantage of methods based on the Pechukas force is the required iterative procedure for the quantum force calculation. In search of the ideal nonadiabatic algorithm yet another method was proposed [102]. This method combines stochastic surface hopping (MDQT) with the mean field force. It is based on the notion that the limitation of the system to pure (adiabatic) states (as is done in MDQT) of the system may not be correct in extended regions of nonadiabatic coupling. The method uses a combination of mean field propagation between hops and projection onto a single adiabatic state when the mean field approximation becomes invalid. The fewest switches hopping criterion ensures the correct branching of classical trajectories, while the mean field force,

$$\mathbf{F}^{MF}(\mathbf{R}(t)) = -\langle \alpha(t, t_i) | \nabla_{\mathbf{R}} H_q(\mathbf{r}, \mathbf{R}(t)) | \alpha(t, t_i) \rangle$$

(Eq. (12)), provides the "best" classical trajectory accompanying the quantum evolution (just like the Pechukas force). This method has been applied to model systems (the same models that were used to test MDQT originally) and results show that in this case this method works better than other methods based on an adiabatic force without increase in computational effort. An advantage is that the classical trajectories are robust with respect to the quantum representation (adiabatic vs diabatic representation), a virtue it inherited from a mean field description. This method appears to have combined two virtues: a simple and intuitive force calculation, and a correct description of branching processes.

2.10. *Quantum Decoherence*

Quantum decoherence is an important issue in mixed quantum/classical simulations. The total wavefunction for system plus bath (Eqs. (2), (16)) has a phase to which both fast and slow degrees of freedom contribute. Upon taking the classical limit for the slow degrees of freedom, the phase information for this part of the system is lost. This phase information is important, however, since it influences the branching ratios of the trajectories. For times shorter than the decoherence time there is interference between the wavefunctions of the slow degrees of freedom for the different possible trajectories. For longer times, the different possible trajectories diverge and there no longer is interference between these different trajectories. This is known as quantum decoherence. In mixed quantum/classical simulations, however, these interference effects are included in an approximate way or not at all. For a more rigorous investigation of quantum decoherence effects, methods which rely on a semiclassical treatment [34, 35] rather than a classical one are obviously better suited.

In MDQT one averages over an ensemble of trajectories, which naturally washes out the coherence within the quantum subsystem, but this does not account for the decoherence effects of the classically treated subsystem. This arises because when one averages over an ensemble of trajectories, one is averaging over probabilities, neglecting interference between the quantum amplitudes of different trajectories. This is the independent trajectory approximation mentioned earlier in Section 2.7. Since MDQT is a mixed quantum/classical method, this is rigorous, but obviously neglects possibly important effects such as nuclear tunneling.

The WRF method explicitly includes a time interval. It is typical (although not necessary) to drop the phase factors of the quantum amplitudes at the end of each time interval. This way an explicit decoherence time is included. (Note that in WRF averaging over initial conditions is necessary as in MDQT.) Typically the decoherence time is chosen equal to the classical time step. The choice of this time step is a rather subtle matter. Since the WRF method relies upon interpolation of the potential energy surface within one classical time step, the time step should be chosen small enough so that interpolation is a reasonable approximation. On the other hand, the time step should not be shorter than the time scale of the coherent dynamics of interest; see, e.g., [78, 103].

The interaction between the system and the bath dictates length and time scales for quantum decoherence [79, 104]. It is possible to estimate this decoherence time scale for the classical degrees of freedom and use this as the time step in the WRF method in order to approximate the effect of the quantum character of the classically treated degrees of freedom. Recently Bittner and Rossky [79, 105] developed a method to incorporate the quantum coherence loss in simulations of mixed quantum/classical systems. This method includes characteristic time and length scales that characterize the decay in coherence due to the differences in bath dynamics for each possible quantum state. It has been tested on a nonadiabatic model charge transfer reaction and shows that a shorter decoherence time scale diminishes the nonadiabaticity, recovering adiabatic dynamics in the limit of rapid decoherence.

In recent work [103, 106] (note that the latter paper corrects an error in the former) the same authors estimated the decoherence time scale on the fly for the hydrated electron system. Their method is based on the frozen Gaussian approach by Heller [107] (to incorporate nuclear tunneling effects), and the work of Neria and Nitzan [108, 109]. The nuclear decoherence time is estimated from the overlap of wave packets evolved on the different effective energy surfaces of the system. It is important to note that the decoherence time is not constant during a single trajectory, let alone for different trajectories. Also, for each pair of states a different decoherence time applies. With extra effort it is in principle possible to determine these decoherence times on the fly for each trajectory. The use of a single decoherence time in simulations is a further approximation. Based on the above simulations the authors determined an average decoherence time for an electron in water and heavy water, and used that as the decoherence time in WRF simulations. Using this methodology they were able to explain the anomalous isotope effect that is observed in water for the nonadiabatic transition rate. Based on the difference in mass between H_2O and D_2O only, one would expect the transition rate to be twice as fast in water as in heavy water. The fact that the dynamics on average evolves coherently for twice as long in D_2O, however, balances this effect and almost no isotope effect is observed, as is seen experimentally [110, 111].

In summary, the nonadiabatic mixed quantum/classical methods presented in these sections mainly differ in the time propagation of the wavefunctions, the force calculation, and the treatment of quantum decoherence. Obviously other mixed quantum/classical methods than the ones discussed here have been developed as well; see, e.g., [112–117].

2.11. *Application: The Hydrated Electron*

The literature devoted to the hydrated electron is extensive. Despite all the studies that have been carried out, however, many features of the hydrated electron, including some of the basic physics, are not yet entirely understood. It is common to invoke a close

analogy to simple solvated anions. One assumes that a cavity in the solvent is occupied by the excess electron, which is surrounded by favorably oriented water molecules. Structural aspects of interest include the size and geometry of the cavity, and the solvation structure. Spectral properties are also of great interest and have been measured experimentally [118–125].

The hydrated electron system is a good candidate for mixed quantum/classical treatment and the simulations of a solvated electron are numerous. Earlier work dealt with the problem within the adiabatic approximation (see, e.g., [65, 66, 126–129]) and was in part able to

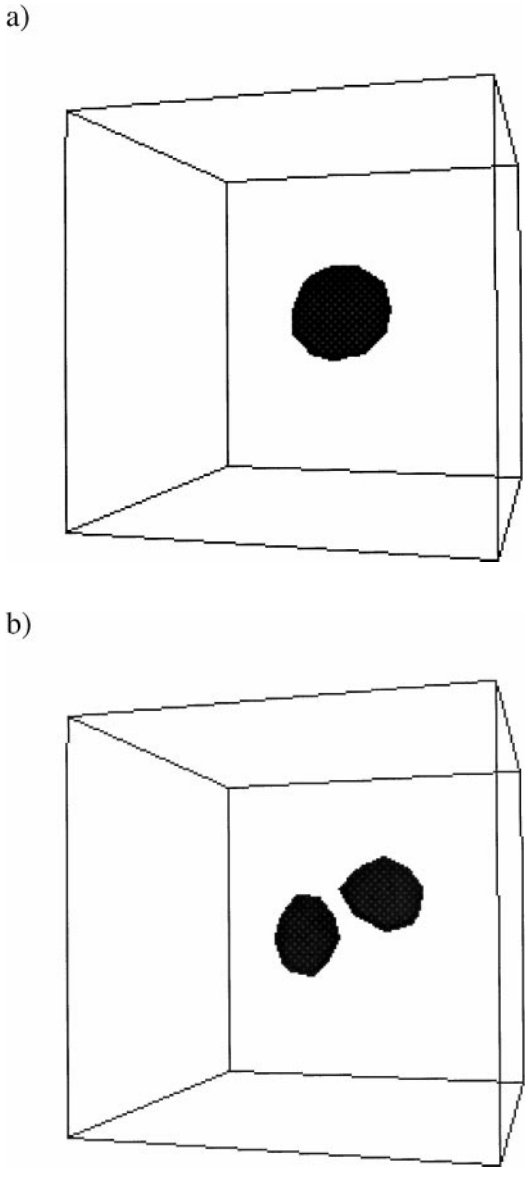

FIG. 5. Electron density in water for the lowest four adiabatic eigenstates: (a) ground-state density; (b)–(d) first three excited states. Isosurfaces of 10% of the density are shown. The electron wavefunctions are represented on a grid and the water molecules are omitted for clarity.

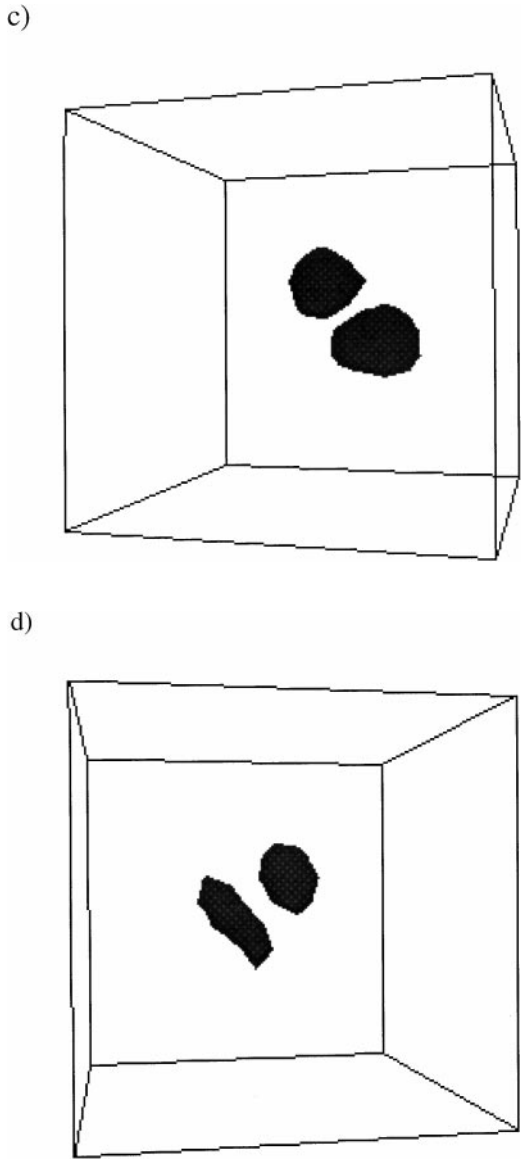

FIG. 5—*Continued*

reproduce and explain experimental spectral properties. It was postulated that inclusion of excited states and nonadiabatic events is essential to reproduce the experimentally observed absorption spectra. When nonadiabatic methods gained interest it was shown that features in the absorption spectrum are indeed due to nonadiabatic transitions (see, e.g., [67–71, 78, 130, 131]).

Structural information about the hydrated electron is plentiful. It is known from both experiment and computer simulation that the eigenstates lowest in energy are self-trapped and occupy only a small volume fraction of the total volume while higher excited states are more extended. Typical electron densities for the instantaneous adiabatic eigenstates lowest in energy of an equilibrated excess electron in water at room temperature are shown in Fig. 5. From simulations one learns that the equilibrium ground state is a nearly spherical

s-like state while the first three excited states are nondegenerate *p*-like states located in the same cavity as the ground state. We estimated the radius of the equilibrated ground-state cavity to be 3.1 ± 0.1 Å from the participation ratio [92]. The excluded volume effect is also reflected in the ground-state radial distribution functions $g_{e^- - \mathrm{O}}$ and $g_{e^- - \mathrm{H}}$. The coordination numbers for oxygen and hydrogen atoms around the electronic center of mass indicate that the water molecules are bond oriented rather than dipole oriented around the electronic density.

Dynamical information is also obtained relatively straightforwardly in time-dependent simulation methods. Nonadiabatic simulation methods allow one to obtain dynamical information for processes in which multiple quantum states play a role. This dynamical information relates to experimentally observed spectra. For example, in order to simulate and study relaxation after photoexcitation one can inject the electron into the excited state of a water configuration and investigate the relaxation process to the ground state. A possible evolution path of the adiabatic energies after injection of the electron in an excited state is illustrated in Fig. 6. This kind of information is not directly obtainable from experiments. Also note the extremely short time scale of the dynamics. In the relaxation one sees different types of interaction. Differences in coupling between states leads to a competition between different relaxation channels. About half of the trajectories show a rapid cascade through the manifold of states down to the ground state, while in the other trajectories the first excited state remains occupied for a considerable time (comparable to or longer than shown in Fig. 6). The latter observation explains features in the experimental absorption spectrum that were not understood before.

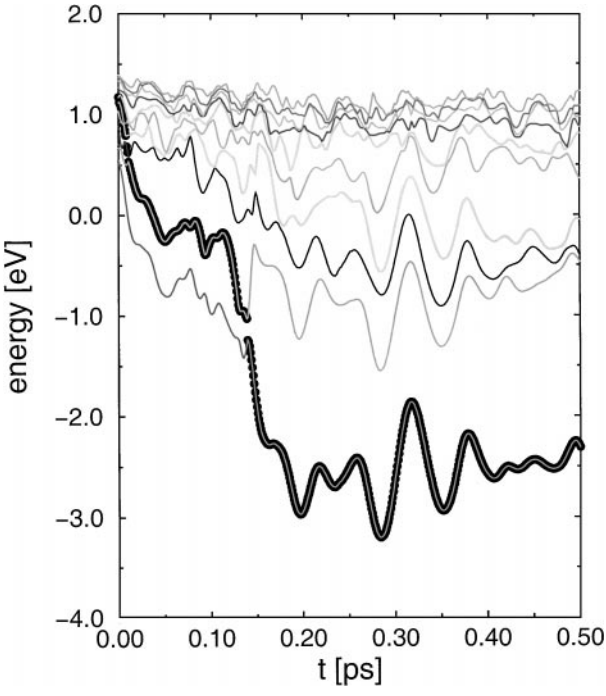

FIG. 6. Example of relaxation dynamics after injection into an excited state. The adiabatic energies are shown as a function of time and the occupied state is marked with a circle. This simulation was done with the MDQT method.

3. SURFACE HOPPING AND THE SIMULATION OF INFREQUENT EVENTS

3.1. *Methods*

In some reactions the energy barrier that has to be overcome to evolve from reactants to products is so high that the reaction rate is extremely low. Dynamical simulation of this type of system requires a different approach from straightforward trajectory integration. A trajectory that is started at the reactant side generally stays there for a very long time before it reaches the energy barrier. The fluctuations in energy in the system are so small with respect to the barrier height that a trajectory reaching the top of the barrier is an infrequent event. For the study of infrequent events it is not feasible to start a trajectory in the reactant region and hope it will eventually go over the barrier and end up at the product region. This is computationally prohibitive even for the most patient. Some tricks have to be invented to deal with this [132–135]. Recently a new method has been developed for this purpose for mixed quantum/classical systems [136]; it is called "multiple potential energy surface–molecular dynamics of infrequent events" (MPES-MDIE). The objective in creating this method was to develop a method to simulate infrequent events that gives the same results as "ordinary" MDQT at a considerably lower computational cost. The basis of this method is transition state theory (TST), originally developed by Wigner, combined with MDQT; not only rate constants but also real-time dynamical properties of reaction mechanisms can be obtained.

It has long been known from classical simulations that simulation of infrequent events is feasible only when trajectories are started at or near the dividing surface S (see, e.g., Ref. [137]). The dividing surface is defined to separate reactants from products and in transition-state theory the equilibrium flux through this dividing surface determines the rate constant. Typically the dividing surface is chosen to be located at or near the top of the energy barrier for the ground state. In the following it is assumed that this dividing surface is the same for all quantum states. Instead of considering a "straightforward" trajectory evolving from reactants to products, we split the trajectory into two parts. The trajectory is started at the dividing surface. The first part of the trajectory is obtained by integrating backward in time from the dividing surface to the reactant region. The second part is obtained by forward integration in time to the product region. The forward and backward parts of the trajectory combine into the complete trajectory.

In the original formulation of TST, recrossings of the dividing surface are not allowed so the dividing surface is crossed once and only once in a reactive event. TST can be straightforwardly reformulated to allow recrossings of the dividing surface, however, and the dynamical factor F accounts for recrossings. The dynamical factor F is obtained from the number of times the dividing surface is crossed in a complete trajectory. The rate constant then is a product of the equilibrium flux through the dividing surface and the dynamical factor. Originally TST only dealt with a single potential energy surface but multiple potential energy surfaces can be included straightforwardly, as was done for the development of MPES-MDIE.

Starting a trajectory "somewhere in the middle," however, is not trivial when stochastic surface hopping is used because this method has a memory: The nature of the quantum wavefunction cannot be determined without knowing the history of the trajectory. The quantum amplitude of each adiabatic state (22), which state is occupied, and the transition probabilities g_{jk} (26) (or $T_{\beta\alpha}$ when using a WRF-like surface hopping method) at a given time all depend on the history of the trajectory. Naively starting with a pure state at the barrier, i.e., a δ-function for the expansion coefficients (and hence occupation probabilities),

is not correct and, moreover, results in a dependence of the rate constant on the choice of the dividing surface S. These problems are overcome in MPES-MDIE by the use of a modified hopping probability f_{jk} in the backward part of the trajectory. This local hopping probability depends neither on history nor on the quantum amplitudes. Because f_{jk} does not have a memory the quantum probabilities can be chosen as a δ-function for the starting configuration near the barrier.

It is obvious that trajectories obtained with a modified hopping probability are different from those that would have been obtained with MDQT but the correct results can be recovered. Assume we are interested in one particular trajectory. The initial state n for the backward trajectory is chosen from a Boltzmann distribution (remember that TST is an equilibrium theory) and the expansion coefficients are set to the corresponding δ-function. (Note that surface hopping itself does not strictly obey microscopic time reversibility because the decision of whether a state switch is allowed is based on different classical velocities in a forward and time-reversed trajectory. Therefore one expects that the distribution on top of the barrier is not strictly Gaussian, but the deviations are very small.) The trajectory is integrated backward in time using the local hopping criterion and the "backward" quantum amplitudes until the reactant region is reached. Its steps are retraced exactly forward in time, except that the trajectory is started with the "correct" pure state at $t = 0$. In the retraced trajectory the "original" switching probabilities g_{jk} are calculated at each time step but no actions are taken based on them. The trajectory—the sequence of hops—is assumed to be reversible in time. The transitions in the retraced forward trajectory have to occur at the same times as in the backward trajectory; otherwise the backward and retraced trajectory would diverge. The retraced forward trajectory gives the correct quantum amplitudes and hopping probabilities at the barrier, which are then used to further integrate the trajectory forward in time (using the correct probabilities g_{jk}) until a specified product state is reached.

The correct switching probabilities are determined *a posteriori* for a backward trajectory started at the dividing surface. The starting conditions of the backward trajectories are artificial, however, and the dynamics of the backward trajectories is based on the incorrect switching probabilities so it may or may not represent the true dynamics well. In order to recover the correct dynamics each trajectory is given a statistical weight to indicate how well the trajectory represents the true dynamics. Thus, instead of a single straightforward trajectory a swarm of trajectories starting at the dividing surface is integrated. Each trajectory is weighted to ensure that one obtains the same quantum probabilities at all times from trajectories based on the approximate probabilities f_{jk} as from trajectories integrated with the correct switching probabilities g_{jk}. In order to achieve this the independent trajectories are weighted afterward with a weighting function W that is a product of weighting factors $w(t_l)$ that are calculated on the fly at each time step t_l:

$$W = \prod_l w(t_l). \tag{32}$$

The weighting functions w are determined during the retraced trajectory by calculating

$$\begin{aligned} w(t_l) &= \frac{g_{jk}}{f_{jk}} && \text{when a hop was attempted to state } k \\ &= \frac{1 - \sum_{j \neq k} g_{jk}}{1 - \sum_{j \neq k} f_{jk}} && \text{when no hop was attempted} \end{aligned} \tag{33}$$

at a given time t_l and for occupied state j. Note that the weighting functions do depend on the history of the trajectory. Also note that if a hop is attempted in the backward trajectory at a given time step either there occurs a hop (the hop is successful) or a velocity reversal takes place (the hop is unsuccessful) when using MDQT as the hopping algorithm. This has to be reproduced in the forward retraced trajectory. The choice for the local hopping criterion f_{jk} is in principle arbitrary, but it is desirable to choose it in such a way that it behaves similarly to the original criterion g_{jk}. This minimizes the number of trajectories necessary to obtain statistically significant results.

The explicit retracing of the steps of the backward trajectory can be eliminated in the determination of the weighting function. An alternative way to obtain W is to consider n_{ef} independent sets of backward trajectories simultaneously, where n_{ef} is the number of included states in the expansion (22). The initial amplitudes for the sets of backward trajectories $\mathcal{C}_j^i$ are chosen as a δ-function at the barrier $\mathcal{C}_j^i = \delta_{ij}$ (the superscript i denotes a set of amplitudes and the subscript j indicates the state as usual). Then the linear combination of amplitudes from the backward trajectories that results in the "correct" amplitudes at the reactant region (a δ-function) can be determined from matrix inversion. Again the trajectories are assumed to hop at the same times as the backward ones. This method is computationally more involved than the explicit retracing of the backward trajectory forward in time, which is conceptually more straightforward.

The heart of the MPES-MDIE method is the general strategy for obtaining the dynamical factor by weighing independent trajectories. Although MPES-MDIE has been formulated based on MDQT, in principle other surface hopping methods with memory could be used such as the WRF method [78]. The equilibrium flux can be calculated in a variety of ways as well.

3.2. *Example Application*

So far the infrequent event method MPES-MDIE has been applied to the calculation of the reaction probability and dynamical factor F in a one-dimensional two-state model [136]. This model could easily be solved without application of MPES-MDIE because of its simplicity but it nevertheless served as a useful test case. A wide range of temperatures was considered and the logarithm of the reaction probability was shown to be inversely proportional to the temperature. The dynamical factor F was shown to decrease with temperature, i.e., there are more recrossings at lower temperature, as expected. This method promises to be very useful for simulation of proton and electron transfer reactions, for example, for proton transfer in bulk water. Under equilibrium conditions this is a slow process and the excess proton relocates slowly through the solvent. (Note that this is a completely different problem from the one we will consider in the next section, where we deal with non-equilibrium situations.)

4. SURFACE HOPPING FOR MULTIPLE QUANTUM DEGREES OF FREEDOM

The previous sections dealt with surface hopping methods that can be equally well applied to multiple quantum degrees of freedom as to a single quantum degree of freedom provided that the adiabatic eigenstates of the system can be calculated accurately. The latter is not trivial. The extension to multiple coupled quantum degrees of freedom is challenging because the correlation among the quantum particles must be included in a computationally

tractable way. Methods based on the Feynman path-integral formalism [138–146] have been utilized to treat multiple hydrogen atoms quantum mechanically, but typically these methods employ a transition state theory approximation rather than directly predict real-time dynamical properties (except Ref. [138]).

One method that has been applied to the quantum dynamical simulation of multiple nuclei or vibrational modes is the TDSCF method [73, 147–151]. In TDSCF an N-particle wavefunction is approximated as a single product of N one-particle wavefunctions (compare to Section 2.1). In this way the N-particle time-dependent Schrödinger equation is separated into N coupled single-particle equations of motion, which leads to substantial computational savings. Each quantum particle moves in a time-dependent mean potential that is obtained by averaging over the motion of all of the other quantum particles in the system. The single-particle equations of motion and the mean potentials in which the quantum particles move must be solved self-consistently. In the application of TDSCF to mixed quantum/classical systems (often called the Q-C TDSCF method [149–152]) the classical particles move in a time-dependent mean potential obtained by averaging over the motion of all of the quantum particles in the system. TDSCF has been extended to incorporate correlation among the quantum particles [153–168] using, for example, multi-configurational TDSCF methods [155–164], but not in the context of mixed quantum/classical simulations. One limitation of TDSCF is that it cannot properly describe branching processes, i.e., processes involving multiple pathways going from an initial state to a final one [153, 154] (see Section 2.5). The accurate description of branching processes is critical in proton transfer reactions because typically there are two distinct states of very different character involved (one ionic and one covalent), and the system must accordingly experience different forces from each of these states.

Recently a method for dealing with more than a single quantum degree of freedom in mixed quantum/classical surface hopping simulations was developed [81]. This method was developed for quantum protons or vibrational modes but adaptation for, e.g., quantum electrons is in principle straightforward. The drawbacks of this method are that it is not variational and that it cannot be proven that the Hellmann–Feynman forces are rigorously correct. More recently a variational method was developed based on this method [82]. Both methods are called multi-configurational molecular dynamics with quantum transitions (MC-MDQT). (The older method will be denoted MC-MDQT*.) These methods are based on a self-consistent field calculation of the quantum adiabatic eigenstates. Note that this is a different approach from that used in TDSCF methods discussed previously. The MC-MDQT methods describe branching processes well.

4.1. *Wavefunctions for Multiple Quantum Degrees of Freedom*

So far we have assumed that the adiabatic eigenstates ϕ_i can be calcuated. For a single quantum degree of freedom the one-particle quantum adiabatic eigenstates are standardly expanded in a set of basis functions χ (note that these χ's have nothing to do with those in Section 2.1)

$$\phi_i(\mathbf{r};\mathbf{R}) = \sum_{\alpha=1}^{K} c_{i\alpha}(\mathbf{R})\chi_\alpha(\mathbf{r};\mathbf{R}), \tag{34}$$

where K is the number of basis functions for the quantum particle. The calculation of the adiabatic eigenstates of the Hamiltonian H_q is equivalent to calculation of the expansion

coefficients $c_{i\alpha}$. The energy eigenvalues ϵ_i and eigenfunctions (given by coefficients $\mathbf{c}_i$) are given by the general eigenvalue equation

$$H_q \mathbf{c}_i = \epsilon_i S \mathbf{c}_i, \tag{35}$$

where H is the $K \times K$ Hamiltonian matrix with elements $\langle \chi_\alpha | H | \chi_\beta \rangle$ (where again $\langle\,\rangle$ stands for integration over the quantum coordinates), and the overlap matrix S has elements

$$S_{\alpha\beta} = \langle \chi_\alpha \mid \chi_\beta \rangle. \tag{36}$$

The eigenvalues ϵ_i and eigenfunctions ϕ_i, $i = 1, \ldots, K$, are obtained by diagonalization of the Hamiltonian matrix. Depending on the basis set size and the nature of the problem there are many ways to calculate (some of) these solutions to the time-independent Schrödinger equation [63, 65, 78, 169–175].

For N quantum particles, the total quantum wavefunction ψ is expanded in a basis of instantaneous adiabatic eigenstates of the quantum Hamiltonian H_q, which are now multiparticle wavefunctions Φ_i,

$$\psi(\mathbf{r}, \mathbf{R}, t) = \sum_i c_i(t) \Phi_i(\mathbf{r}; \mathbf{R}(t)). \tag{37}$$

The N-dimensional eigenvalue equation (time-independent Schrödinger equation) that has to be solved is

$$H_q(\mathbf{r}, \mathbf{R}) \Phi_i(\mathbf{r}; \mathbf{R}) = E_i(\mathbf{R}) \Phi_i(\mathbf{r}; \mathbf{R}). \tag{38}$$

(N-dimensional refers to the number of quantum degrees of freedom. Each quantum degree of freedom may be m-dimensional, $m = 1, 2, 3$, so technically the set is Nm-dimensional.) In a straightforward N-dimensional generalization of MDQT the N-particle adiabatic states are expanded in N-dimensional basis functions analogous to the expansion in the one-particle case. This approach is called a complete configuration interaction (CI) treatment, and here for N quantum degrees of freedom the basis set expansion is

$$\Phi_i(\mathbf{r}; \mathbf{R}) = \sum_J^K c_{iJ}(\mathbf{R}) \xi_J(\mathbf{r}; \mathbf{R}), \tag{39}$$

where K is the number of N-dimensional basis functions ξ_J. The N-particle basis functions ξ_J are products of the one-particle basis functions $\chi_{j_k}^{(k)}$,

$$\xi_J(\mathbf{r}; \mathbf{R}) = \prod_{k=1}^N \chi_{j_k}^{(k)}(\mathbf{r}_k; \mathbf{R}), \tag{40}$$

where the superscript (k) labels the quantum degrees of freedom, $1, \ldots, N$. Note that $j = (j_1, \ldots, j_N)$ is a set of indices where j_k is one of the K_k basis functions for quantum particle k. For example, for two quantum degrees of freedom the index $J = (1, 1)$ denotes the basis function $\xi_{(1,1)} = \chi_1^{(1)} \chi_1^{(2)}$, a product of the basis functions $\chi_1^{(1)}$ and $\chi_1^{(2)}$. (A commonly used notation for such a product is $\chi_1^{(1)} \otimes \chi_1^{(2)}$.) In Eq. (39) the total number of N-dimensional basis functions equals $K = \prod_{k=1}^N K_k$, where K_k is the number of

one-particle basis functions for quantum particle k. Note that the formalism is presented in terms of Hartree products because it is assumed that the quantum particles occupy entirely different regions in space. This method can be generalized by using Slater determinants.

When one uses a complete CI expansion of the total wavefunction (39), solving the time-independent Schrödinger equation quickly becomes computationally intractable with increasing number of quantum particles N and number of N-particle basis functions. This problem can be surmounted by using a self-consistent field (SCF) formulation. In a self-consistent field approach, the total N-dimensional eigenvalue equation for the N-dimensional adiabatic states is split into a set of one-dimensional coupled equations for one-particle adiabatic eigenstates ϕ_i. The N-particle adiabatic states Φ_i can be obtained either in a single-configurational (SC-SCF) method or a multi-configurational (MC-SCF) method. A configuration in this context denotes a product of single-particle adiabatic states ϕ_k. In a single configuration method each adiabatic state of the total system is approximated by a single product of one-particle wavefunctions. The approximation of the adiabatic states by single configurations is given by

$$\Phi_i(\mathbf{r};\mathbf{R}) = \xi_J(\mathbf{r};\mathbf{R}) \equiv \prod_{k=1}^{N} \phi_{j_k}^{(k)}(\mathbf{r}_k;\mathbf{R}). \tag{41}$$

Here, J is a set of indices defining the configurations $J = (j_1, j_2, \ldots, j_N)$ and j_k is the state of quantum particle k belonging to the N-particle configuration ξ_J. Here an index $J = (1, 1)$ denotes the configuration $\xi_{(1,1)} = \phi_1^{(1)}\phi_1^{(2)}$. A single configuration description results in easy-to-solve equations, but fails to include important correlation between the quantum particles [153, 154] as expected (Sections 2.1 and 2.5).

In order to accurately incorporate quantum correlation, a multi-configurational method is needed (compare to Section 2.6). A multi-configurational description leads to more complicated equations. The adiabatic eigenstates are expanded in a basis of Q configurations, i.e., they are a mixture of configurations ξ_J,

$$\Phi_i = \sum_{J}^{Q} d_{iJ}(\mathbf{R})\xi_J(\mathbf{r};\mathbf{R}) \tag{42}$$

$$= \sum_{j_1=1}^{m_k} \cdots \sum_{j_N=1}^{m_k} d_{ij_1,\ldots,j_N}(\mathbf{R})\phi_{j_1}^{(1)}(\mathbf{r}_1;\mathbf{R}) \cdots \phi_{j_N}^{(N)}(\mathbf{r}_N;\mathbf{R}). \tag{43}$$

Here the d_{kJ}'s are the so-called configuration interaction coefficients, m_k is the number of one-particle states for a given particle k, and Q is the number of included configurations $Q = \prod_{k=1}^{N} m_k$. If a complete basis were used, the expansion would approach the exact wavefunction. In practice, however, the summation is limited.

4.2. *Multi-configurational Molecular Dynamics with Quantum Transitions*

Self-consistent calculation of the adiabatic eigenstates Φ_i as described above is straightforwardly combined with MDQT for incorporation of nonadiabatic dynamics. In the original formulation of multi-configurational molecular dynamics with quantum transitions (MC-MDQT*) [81] the multi-configurational approach to the total wavefunction is combined with the use of effective Hamiltonians. Each quantum particle "feels" an effective Hamiltonian h_{eff} in which the interactions are averaged over the wavefunctions of all other quantum

particles. Then the set of equations

$$h_{\text{eff}}^{(k)}(\mathbf{r}_k, \mathbf{R})\phi_i^{(k)}(\mathbf{r}_k; \mathbf{R}) = \epsilon_i^{(k)}(\mathbf{R})\phi_i^{(k)}(\mathbf{r}_k; \mathbf{R}) \tag{44}$$

has to be solved self-consistently, where each equation is solved in the same manner as for a single quantum degree of freedom. The effective Hamiltonian for particle k and occupied state Φ_i is given by

$$h_{\text{eff}}^{(k)} = t_k + \sum_J^Q d_{iJ}^2 \left\langle \prod_{k' \neq k}^N \phi_{j_{k'}}^{(k')}(\mathbf{r}_{k'}))|V(\mathbf{r}, \mathbf{R}, t)| \prod_{k' \neq k}^N \phi_{j_{k'}}^{(k')}(\mathbf{r}_{k'})) \right\rangle, \tag{45}$$

where t_k is the kinetic energy operator for this particle k, and the second part of the equation is the effective potential energy surface for this particle when state i is occupied. An example of effective potential energy surfaces for two one-dimensional quantum protons is given in Fig. 7, where in addition to the effective potential energy curves also the lowest two

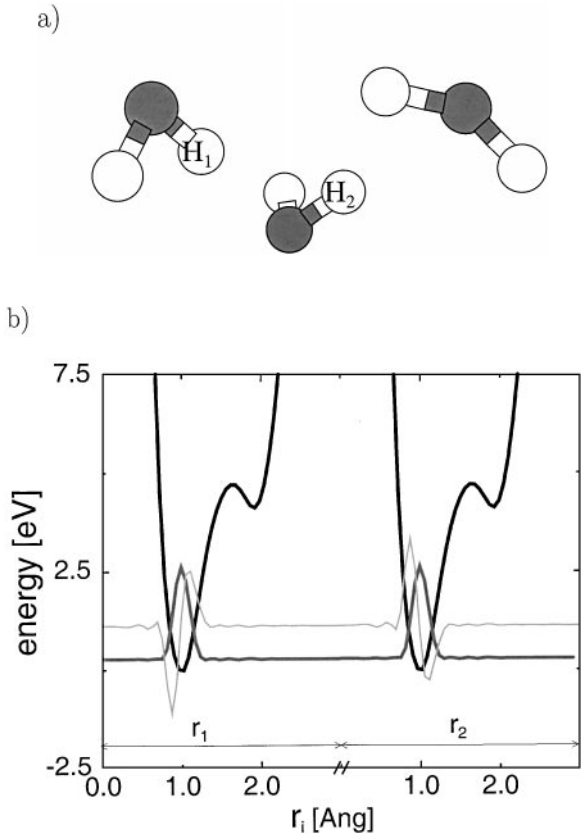

FIG. 7. (a) Chain of three water molecules in which hydrogens that form hydrogen bonds within the chain are described quantum mechanically (and labeled H_1 and H_2) while all other degrees of freedom are treated classically. H_1 and H_2 are restricted to one-dimensional motion on the donor–acceptor axes in this example. For illustrative purposes the quantum protons are placed at the expectation values of their coordinates in this kind of figure. (b) One-dimensional effective potential for each quantum proton with two eigenstates lowest in energy as a function of quantum coordinates r_k along the oxygen–oxygen axes.

one-particle adiabatic eigenstates are depicted for each particle. The use of this effective Hamiltonian provides a clear physical picture of the proton transfer mechanisms. The system is in a single configuration far from regions of strong coupling, while only in regions of strong coupling the are wavefunctions multiconfigurational.

MC-MDQT* describes branching processes well and it was applied to a simple one-dimensional model systems of proton transfer reactions with up to three quantum protons. It was shown that this method is accurate and fast for these systems. The occupation probabilities of the eigenstates and the fraction of trajectories in each state at a given time were compared to results from a complete CI calculation for two quantum protons and were in excellent agreement. MC-MDQT* is not a variational method, however, and one cannot rigorously prove that the Hellmann–Feynman forces equal the exact forces. Although the Hellmann–Feynman force is identical to the exact force for the exact wavefunction (see Eq. (12)–(14)), it has been shown to differ from the exact force for some types of approximate wavefunctions [176, 177]. As a result, Pulay derived corrections to the Hellmann–Feynman force for electronic wavefunctions [176, 177]. The analogous correction terms for proton (or vibrational) wavefunctions are numerically difficult to calculate with the MC-MDQT* method. In general calculation of these Pulay corrections may not be easy or may even be computationally prohibitive if an analytical expression cannot be derived.

In the newer MC-MDQT method both of the above problems are addressed. It is a variational method and it was proven that the Hellmann–Feynman forces are exact under certain conditions. For details see Ref. [82]. The adiabatic eigenstates are again expanded according to Eq. (42). In order to determine the total N-particle wavefunction and the one-particle adiabatic eigenstates, or in other words to calculate the coefficients d_{nJ} and $c_{i\alpha}^{(k)}$, the variational principle is applied to the total energy of all n adiabatic states $E_n = \langle \Phi_n | H_q | \Phi_n \rangle$. This is done subject to the orthonormality conditions for the one-particle states

$$\left\langle \phi_i^{(k)} \,\middle|\, \phi_j^{(k)} \right\rangle - \delta_{ij} = 0 \tag{46}$$

or

$$\sum_{\alpha\beta}^{K_k} c_{i\alpha}^{(k)} c_{j\beta}^{(k)} S_{\alpha\beta}^{(k)} - \delta_{ij} = 0, \tag{47}$$

where $S_{\alpha\beta}^{(k)}$ is the overlap matrix of the basis functions χ, and that for the configurations

$$\sum_{J=1}^{Q} d_{nJ}^2 - 1 = 0 \tag{48}$$

for all n eigenstates. From now on we will drop the subscript denoting the adiabatic state n since all the sub- and superscripts in the following tend to be confusing as it is. The equations below are for a given adiabatic state, and for each adiabatic state analogous equations apply. Equations (47) and (48) lead to the sets of equations

$$\frac{\partial}{\partial d_L}\left[E - \eta\left(\sum_J^Q d_J^2 - 1 \right) \right] = 0 \tag{49}$$

and

$$\frac{\partial}{\partial c_{l\lambda}^{(k)}}\left[E-\sum_{ij}^{m_k}\epsilon_{ij}^{(k)}\left(\sum_{\alpha\beta}^{K_k}\left(c_{i\alpha}^{(k)}c_{j\beta}^{(k)}S_{\alpha\beta}^{(k)}\right)-\delta_{ij}\right)\right]=0, \tag{50}$$

when η and the $\epsilon_{ij}^{(k)}$'s are Lagrange multipliers. The first set of equations reduces to the standard eigenvalue equation

$$\mathbf{Hd}=\eta\mathbf{d}, \tag{51}$$

where the matrix $\mathbf{H}$ has matrix elements $H_{IJ}\equiv\langle\xi_I|H_q|\xi_J\rangle$. As in standard electronic structure theory, the coefficients d_I can be calculated by diagonalizing the $\mathbf{H}$ matrix. The second set of equations can be written as a matrix equation from which the $c_{i\alpha}^{(k)}$ coefficients, i.e., the one-particle adiabatic eigenstates, can be calculated [178].

The MC-MDQT method as implemented is a multi-grid method. The wavefunctions of each quantum degree of freedom are represented on a grid that is defined by the positions of two classical particles (donor and acceptor). The quantum Hamiltonian depends on both quantum and classical degrees of freedom (i.e., $H_q(\mathbf{r},\mathbf{R},t)$), and the coefficients depend on the classical degrees of freedom (i.e., $d_J(\mathbf{R})$ and $c_{i\alpha}^{(k)}(\mathbf{R})$). In addition, each basis function $\chi_\alpha^{(k)}$ depends on a set of parameters $p_{\alpha\nu}^{(k)}$ (including, for example, the center and the width), which may depend explicitly on the classical degrees of freedom. The expression for the force is then for each component R_μ, where μ indicates both a classical particle and a component (i.e., x, y, or z):

$$\begin{aligned}F_{R_\mu}&=-\frac{\partial E(\mathbf{R})}{\partial R_\mu}\\&=-\frac{\partial}{\partial R_\mu}\left\langle\Phi\left(d_J,c_{i\alpha}^{(k)},p_{\alpha\nu}^{(k)}\right)|H_q(\mathbf{r};\mathbf{R})|\Phi\left(d_J,c_{i\alpha}^{(k)},p_{\alpha\nu}^{(k)}\right)\right\rangle.\end{aligned} \tag{52}$$

It was shown that with an appropriate choice of basis functions the Hellmann–Feynman force (12) is rigorously identical to the exact force in MC-MDQT [82]. There are two conditions that the basis functions $\chi_\alpha^{(k)}$ need to satisfy in order to achieve this. (Note that these are sufficient but not necessary conditions.) The first condition is that the origin for the basis functions $\chi_\alpha^{(k)}$ for quantum particle k exactly follows the motion of the classical particles associated with this quantum particle. The second condition is that the basis functions depend only on the distance to the origin of the basis function and other constant parameters, such as the width, that do not depend on the classical coordinates. In this manner the expensive calculation of Pulay corrections is avoided.

In practice a way to initialize the MC-MDQT method at every time step is required. In principle one could use the values from a previous time step as a starting point for the self-consistent calculations, but this requires quite a large number of configurations in order to obtain sufficient flexibility in the wavefunctions. Alternatively the MC-MDQT* method can be used as a startup. For the systems we studied the initial wavefunctions calculated by MC-MDQT* needed only little refinement. Apart from the multi-configurational mixing that occurs during branching processes, in most instances the wavefunctions could be accurately described by a single configuration. Although more complicated to program, convergence with the MC-MDQT method is slightly faster than with the MC-MDQT* method.

4.3. *Application: Proton Transport along Water Chains*

Reactions in which multiple protons are transfered play a critical role in many important chemical and biological processes, for example, a wide range of enzyme reactions (see, e.g., [179–182]. Moreover, in transmembrane proteins such as bacteriorhodopsin [183, 184] and photosynthetic reaction centers [185, 186], protons are transported across a membrane through a series of proton transfer steps involving water molecules and the side chains of amino acid residues in the protein. In this section we focus on proton transport along chains of hydrogen-bonded water molecules, which is thought to play an important role in the fast translocation of protons over large distances in these proton pumps [187].

A number of simulations of proton transfer reactions in solution have been done; see, e.g, [139–146, 152, 188–202]. Most of the studied proton transfer reactions are single-proton transfer reactions, where only one hydrogen atom is treated quantum mechanically, and are not easily extendable to processes involving coupled multiple proton transfer steps, where many hydrogen atoms must be treated quantum mechanically. Recently numerous simulations of proton transfer in water have been performed [138, 145, 146, 203–206]. In particular, Pomès and Roux used Feynman path-integral methods to study the equilibrium properties of protonated chains of water molecules [145, 146], and Lobaugh and Voth used the centroid molecular dynamics method to study the dynamics of a single-proton transfer reaction in water [138]. The work summarized here differs from previous work in that quantum dynamical non-equilibrium simulations of multiple proton transfer reactions in chains of water molecules were performed using the MC-MDQT method [207–209]. Proton transfer along protonated chains in an external electrical field of three and four water molecules was investigated. A protonated chain of four water molecules is thought to be responsible for the proton shuttle mechanism in the bacteriorhodopsin proton channel. In order to drive the proton transfer process the effects of the protein on the chain of water molecules were mimicked. A linearly increasing external electric field was applied to the water chain to model the field exerted by a protein, and harmonic restraints were applied to the oxygen atoms to model the structural constraints of the protein. Only the transferring hydrogen atoms (two or three in this case) were treated quantum mechanically due to computational limitations arising from the need to calculate multidimensional integrals for the many-body polarization terms in the employed water potential model [210–212]. For further details see Ref. [207]. Note that in these simulations the system was in its electronic ground state, while the protons were doing the nonadiabatic dynamics.

The MC-MDQT method was tested on a protonated chain of three water molecules where two protons were treated as one-dimensional quantum particles [82]. The simulations were initiated in configurations where the excess proton had been stabilized on one end of the chain by an external electric field. In these initial simulations themselves, however, the external field was turned off at time $t = 0$. The agreement between the energy eigenvalues obtained by a full CI calculation and MC-MDQT (which is an order of magnitude faster) was excellent for the four adiabatic states lowest in energy when only nine configurations were used in MC-MDQT. The forces were also in excellent agreement.

In subsequent simulations, the external field was ramped in order to drive the proton transfer process. The effect of the ramping rate and the strength of the harmonic restraints on the oxygen atoms, i.e., the stiffness of the chain due to structural constraints of the protein, on the transfer rates and the importance of excited states in the dynamics were

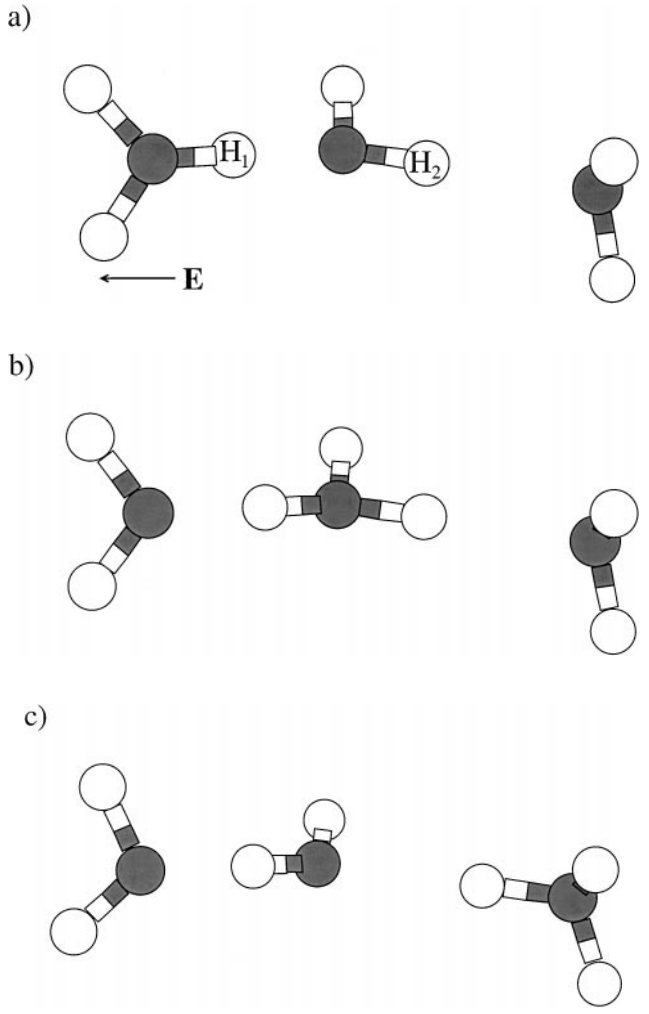

FIG. 8. Snapshots of configurations during a sample trajectory of the protonated trimer with harmonic restraints force constant $k_s = 150$ kcal mol^{-1} Å^{-2} and ramping rate $\Delta E = 10^6$ V cm$^{-1}\Delta t^{-1}$ at times (a) $t = 0.000$ fs, (b) $t = 3.125$ fs, and (c) $t = 9.375$ fs. ($\Delta t = 0.0625$ fs.) Note that for the initial non-equilibrium configuration the applied electric field $|E| = 5 \times 10^7$ V/cm points toward the left end of the chain in order to keep the quantum protons, H_1 and H_2, in place. The applied field is then increased linearly in time during the trajectory.

investigated. In Fig. 8 an example trajectory is shown for the protonated trimer. In all trimer trajectories a sequential mechanism was observed at early times in the evolution.

In these simulations, the ramping rate of the external field directly controlled the transfer process. It was observed that the transfer process is direct and fast for rapid ramping of the external field, whereas the transfer process is more indirect and involves alternative pathways for slow ramping rates. This affects the importance of nonadiabatic events. For the highest ramping rates the process was primarily adiabatic. Only for the slowest ramping rate were nonadiabatic effects considerable. Nonadiabatic events were mainly observed after the maximum value for the external field was reached and the second proton moved back and forth around its midpoint before forming a new OH bond. Nonadiabatic dynamics did not become important until after the transfer process was completed, however.

Another factor that influences the importance of nonadiabatic dynamics is the flexibility of the chain. Different stiffnesses were investigated ranging from an entirely flexible chain to a very stiff chain. Increased flexibility of the chain increased nonadiabatic effects for a given ramping rate of the external field. This phenomenon arises in part from the larger temperature increase for more flexible chains. For the protonated tetramer the same trends were observed.

These simulations indicate that the fluctuating electric fields and structural restraints of the protein environment strongly affect the dynamics of proton transport along water chains. In addition, these simulations illustrate that nonadiabatic effects play an important role in the proton transfer dynamics of water chains under certain non-equilibrium conditions. Nonadiabatic effects may not be as important in proteins such as bacteriorhodopsin, however, because of thermal dissipation. Moreover, nonadiabatic effects may not play a significant role in the protein environment because the proton is quickly transferred to an amino acid after moving down the water chain. The MC-MDQT method is currently used to study the dynamical effects of solvation by solvating various parts of the chain with explicit water molecules [213]. Moreover, MC-MDQT will be used to study proton transport along a water chain in bacteriorhodopsin to investigate the structural and dynamical effects of a specific protein environment.

5. SUMMARY

In this paper mixed quantum/classical methods were discussed for computer simulation of nonadiabatic dynamics, i.e., of processes in which excited states play a prominent role. The methods summarized here all recognize the fact that a mixed-state description of the quantum subsystem is often correct only for very short time scales. The methods hence all use various surface hopping algorithms to overcome the problems associated with mixed-state propagation for longer time scales. At this point no conclusive evidence is known as to which method is the best.

The advantages of the MDQT method [1] are that the forces are easy to evaluate and that the correct occupation probabilities of the quantum states are obtained. A disadvantage for complicated systems is that an ensemble of trajectories has to be integrated in order to damp the quantum coherence. A decoherence time or a coherence damping factor could be defined explicitly but clashes to some extent with the philosophy of this method. So far the coherence is dropped only rarely in applications of this method. The advantage of most methods based on the Pechukas force [78, 100] is that an explicit decoherence time is defined so that less averaging over trajectories is needed. Also the quantum character of the classical particles can be partially included in this way. This can also be seen as a disadvantage, however: Defining a decoherence time is tricky. Not only does it vary during a trajectory, but it also differs between different pairs of states. A definite disadvantage is that the Pechukas force is not predictive and hence the force calculation is far from simple. Another method combines surface hopping with a mean field force for short time scales [102]. Here an advantage is that the force calculation is simple while the combination with the fewest switches criterion from MDQT guarantees that the correct occupation probabilities of the states are obtained. An advantage over MDQT is that this method appears to be more robust with respect to representation (adiabatic vs diabatic), but the latter method has not been extensively tested yet. Obviously all methods discussed do require averaging over initial conditions.

In addition we summarized methods based on combination of MDQT with other techniques. The first is a combination of MDQT with the ideas of transition-state theory and is a method for simulation of infrequent events. The second is a combination with a multiconfigurational self-consistent field calculation of the adiabatic eigenstates for the simulation of multiple quantum degrees of freedom. Several applications were given as an example.

The field of mixed quantum/classical simulation techniques is far from static. The systems that can be investigated grow with the growing computer power. Mixed quantum/classical treatment will remain the method of choice for many systems for which complete quantum mechanical dynamical treatment remains impossible in spite of increasing computational resources. Semiclassical methods are very promising as well, however.

ACKNOWLEDGMENTS

I thank Sharon Hammes-Schiffer for being a great source of inspiration. I thank her, as well as Simon de Leeuw, for many helpful discussions. George Schatz is acknowledged for a thorough reading of this manuscript and useful comments.

REFERENCES

1. J. C. Tully, Molecular Dynamics with electronic transitions, *J. Chem. Phys.* **93**, 1061 (1990).
2. D. Sprous, M. A. Young, and D. L. Beveridge, Molecular dynamics studies of the conformational preferences of a DNA double helix in water and ethanol/water mixture: Theoretical considerations of the A–B transition, *J. Phys. Chem.* **102**, 4658 (1998).
3. H. J. C. Berendsen, J. M. Postma, W. F. van Gunsteren, and J. Hermans, in *Intermolecular Forces*, edited by B. Pullman (Reidel, Dordrecht, 1981).
4. H. J. C. Berendsen, J. R. Grigera, and T. P. Straatsma, The missing term in effective pair potentials, *J. Phys. Chem.* **91**, 6269 (1987).
5. W. L. Jorgensen, J. Chandtasekhar, J. D. Madura, R. W. Impey, and M. L. Klein, Comparison of simple potential functions for simulating liquid water, *J. Chem. Phys.* **79**, 926 (1983).
6. E. E. Nikitin, *Theory of Elementary Atomic and Molecular Processes in Gases* (Clarendon Press, Oxford, 1974).
7. A. Messiah, *Quantum Mechanics* (Wiley, New York, 1962), Vol. 1, p. 222.
8. A. Selloni, P. Carnevali, R. Car, and M. Parrinello, Localization, hopping, and diffusion of electrons in molten salts, *Phys. Rev. Lett.* **59**, 823 (1987).
9. R. P. Feynman, Space-time approach to non-relativistic quantum mechanics, *Rev. Mod. Phys.* **20**, 367 (1948).
10. R. P. Feynman and A. R. Hibbs, *Quantum Mechanics and Path Integrals* (McGraw–Hill, New York, 1965).
11. D. Chandler and P. G. Wolynes, Exploiting the isomorphism between quantum mechanics and classical statistical mechanics of poly-atomic fluids, *J. Chem. Phys.* **74**, 4078 (1981).
12. M. Parrinello and A. Rahman, Study of an F-center in molten KCl, *J. Chem. Phys.* **80**, 860 (1984).
13. M. Sprik, M. L. Klein, and D. Chandler, Staging: A sampling technique for the MC evaluation of path integrals, *Phys. Rev. B* **31**, 4234 (1985).
14. M. Sprik, M. L. Klein, and D. Chandler, Computer simulation of a quantum particle in a quenched disordered system: Direct observation of Lifschitz traps, *Phys. Rev. B* **32**, 545 (1985).
15. M. Sprik, M. L. Klein, and D. Chandler, Simulation of an excess electron in a hard-sphere fluid, *J. Chem. Phys.* **83**, 3042 (1985).
16. B. J. Berne and D. Thirumalai, On the simulation of quantum systems: Path integral methods, *Ann. Rev. Phys. Chem.* **37**, 401 (1986).
17. R. A. Holroyd and W. F. Smidt, Transport of electrons in nonpolar fluids, *Ann. Rev. Chem.* **40**, 439 (1989).

18. G. J. Martyna and B. J. Berne, Structure and energetics of Xen—Many-body polarization effects, *J. Chem. Phys.* **90**, 3744 (1989).
19. J. P. Hernandez, Electron self-trapping in liquids and dense gases, *Rev. Mod. Phys.* **63**, 675 (1991).
20. J. M. Lopez-Castillo, Y. Frongillo, B. Plenckiewicz, and J. P. Gerin, Path-integral molecular-dynamics calculation of the conduction-band energy minimum V0 of excess electrons in fluid argon, *J. Chem. Phys.* **96**, 9092 (1992).
21. D. Chandler, in *Liquids, Freezing and Glass Transition*, edited by J. P. Hansen, D. Levesque, and J. Zinn-Justin (North-Holland, Amsterdam, 1989), p. 195.
22. E. Gallicchio and B. J. Berne, On the calculation of dynamical properties of solvated electrons by maximum entropy analytic continuation of path integral Monte Carlo data, *J. Chem. Phys.* **105**, 7064 (1996).
23. J. Cao and G. A. Voth, A new perspective on quantum time-correlation functions, *J. Chem. Phys.* **99**, 10070 (1993).
24. J. Cao and G. A. Voth, The formulation of quantum-statistical mechanics based on the Feynman path centroid density. 1. Equilibrium properties, *J. Chem. Phys.* **100**, 5093 (1994).
25. J. Cao and G. A. Voth, The formulation of quantum-statistical mechanics based on the Feynman path centroid density. 2. Dynamical properties, *J. Chem. Phys.* **100**, 5106 (1994).
26. J. Cao and G. A. Voth, The formulation of quantum-statistical mechanics based on the Feynman path centroid density. 3. Phase space formalism and analysis of centroid molecular dynamics, *J. Chem. Phys.* **101**, 6157 (1994).
27. J. Cao and G. A. Voth, The formulation of quantum-statistical mechanics based on the Feynman path centroid density. 4. Algorithms for centroid molecular-dynamics, *J. Chem. Phys.* **101**, 6168 (1994).
28. J. Cao and G. A. Voth, The formulation of quantum-statistical mechanics based on the Feynman path centroid density. 5. Quantum instantaneous normal-mode theory of liquids, *J. Chem. Phys.* **101**, 6184 (1994).
29. G. J. Martyna, Adiabatic path integral molecular dynamics methods. 1. Theory, *J. Chem. Phys.* **104**, 2018 (1996).
30. J. Cao and G. J. Martyna, Adiabatic path integral molecular dynamics methods. 2. Algorithms, *J. Chem. Phys.* **104**, 2028 (1996).
31. M. F. Herman, A semiclassical surface hopping propagator for nonadiabatic problems, *J. Chem. Phys.* **103**, 8081 (1995).
32. T. J. Martinez, M. Ben-Nun, and R. D. Levine, Multi-electronic-state molecular dynamics: A wave function approach with applications, *J. Phys. Chem.* **100**, 7884 (1996).
33. M. Ben-Nun and T. J. Martinez, Nonadiabatic molecular dynamics: Validation of the multiple spawning method for a multidimensional problem, *J. Chem. Phys.* **108**, 7244 (1998).
34. X. Sun and W. H. Miller, Mixed semiclassical–classical approaches to the dynamics of complex molecular systems, *J. Chem. Phys.* **106**, 916 (1997).
35. X. Sun and W. H. Miller, Semiclassical initial value representation for electronically nonadiabatic molecular dynamics, *J. Chem. Phys.* **106**, 6346 (1997).
36. D. E. Skinner and W. H. Miller, Application of the semiclassical initial value representation and its linearized approximation to inelastic scattering, *Chem. Phys. Lett.* **300**, 20 (1999).
37. K. Thompson and N. Makri, Influence functionals with semiclassical propagators in combined forward–backward time, *J. Chem. Phys.* **110**, 1343 (1999).
38. R. Car and M. Parrinello, Unified approach for molecular dynamics and density functional theory, *Phys. Rev. Lett.* **55**, 2471 (1985).
39. D. K. Remler and P. A. Madden, Molecular dynamics without effective potentials via the Car–Parrinello approach, *Mol. Phys.* **70**, 921 (1990).
40. A. Selloni, R. Car, M. Parrinello, and P. Carnevali, Electron pairing in dilute liquid–metal metal halide solutions, *J. Phys. Chem.* **91**, 4947 (1987).
41. K. Laasonen, M. Sprik, M. Parrinello, and R. Car, Ab initio liquid water, *J. Phys. Chem.* **99**, 9080 (1993).
42. G. Onida, W. Andreoni, J. Kohanoff, and M. Parrinello, Ab-initio molecular-dynamics of C-70—Intramolecular vibrations and zero-point motion effects, *Chem. Phys. Lett.* **219**, 1 (1994).

43. D. Marx and M. Parrinello, Ab initio path integral molecular dynamics: Basic ideas, *J. Chem. Phys.* **104**, 4077 (1996).
44. M. P. Allen and D. J. Tildesley, *Computer Simulations of Liquids* (Clarendon Press, Oxford, 1987).
45. D. Frenkel and B. Smit, *Understanding Molecular Simulation. From Algorithms to Applications* (Academic Press, Boston, 1996).
46. C. W. Gear, *Numerical Initial Value Problems in Ordinary Differential Equations* (Prentice Hall, Englewood Cliffs, NJ, 1971).
47. W. C. Swope, H. C. Andersen, P. H. Berens, and K. R. Wilson, A computer simulations method for the calculation of equilibrium constants for the formation of physical clusters of molecules: Application to small water clusters, *J. Chem. Phys.* **76**, 637 (1982).
48. S. W. de Leeuw, J. W. Perram, and E. R. Smith, Simulation of electrostatic systems in periodic boundary conditions. I. Lattice sums and dielectric constants, *Proc. R. Soc. London A* **373**, 27 (1980).
49. H. G. Petersen, D. Soelvason, J. W. Perram, and E. R. Smith, The very fast multipole method, *J. Chem. Phys.* **101**, 8870 (1994).
50. I. G. Tironi, R. Sperb, P. E. Smith, and W. F. van Gunsteren, A generalized reaction field method for molecular-dynamics simulations, *J. Chem. Phys.* **102**, 5451 (1995).
51. B. A. Luty, I. G. Tironi, and W. F. van Gunsteren, Lattice sum methods for calculating electrostatic interactions in molecular simulations, *J. Chem. Phys.* **103**, 3014 (1995).
52. J. P. Ryckaert, G. Ciccotti, and H. J. C. Berendsen, Numerical integration of the Cartesian equations of motion of a system with constraints: Molecular dynamics of n-alkanes, *J. Comput. Phys.* **23**, 327 (1977).
53. S. W. de Leeuw, J. W. Perram, and H. G. Petersen, Hamilton equations for constrained dynamics systems, *J. Statist. Phys.* **61**, 1203 (1990).
54. H. C. Andersen, Rattle: A velocity version of the shake algorithm for molecular dynamics calculations, *J. Comput. Phys.* **52**, 24 (1983).
55. S. Nosé, A Molecular Dynamics method for simulation in the canonical ensemble, *Mol. Phys.* **52**, 255 (1984).
56. S. Nosé, A unified formulation of the constant temperature molecular dynamics methods, *J. Chem. Phys.* **81**, 511 (1984).
57. W. G. Hoover, Canonical dynamics: Equilibrium phase-space dynamics, *Phys. Rev. A* **31**, 1695 (1984).
58. D. J. Evans and B. Lee Holian, The Nosé–Hoover thermostat, *J. Chem. Phys.* **83**, 4069 (1985).
59. H. C. Andersen, M. P. Allen, A. Bellemans, J. Board, J. H. R. Clarke, M. Ferrario, S. Nosé, J. V. Opheusden, and J. P. Ryckaert, *Rapport d'activité scientifique du CECAM* (1984).
60. F. Ancilotto and F. Toigo, Computer-simulations of excess electron-transport in neon, *Phys. Rev. A* **45**, 4015 (1992).
61. H. S. Mei and D. F. Coker, Quantum molecular dynamics studies of H-2 transport in water, *J. Chem. Phys.* **104**, 4755 (1996).
62. A. Nakano, R. K. Kalia, and P. Vanishta, Simulation of many-electron correlations in a resonant-tunneling diode, *Phys. Rev. B* **43**, 10928 (1991).
63. M. D. Feit, J. A. Fleck, and A. J. Steiger, Solution of the Schroedinger equation by a spectral method, *J. Comput. Phys.* **47**, 412 (1982).
64. K. A. Motakabbir, J. Schnitker, and P. J. Rossky, Transient photophysical hole-burning spectroscopy of the hydrated electron—A quantum dynamical simulation, *J. Chem. Phys.* **90**, 6916 (1989).
65. J. Schnitker, K. Motakabbir, P. J. Rossky, and R. Friesner, A-priori calculation of the optical-absorption spectrum of the hydrated electron, *Phys. Rev. Lett.* **60**, 456 (1988).
66. P. J. Rossky and J. Schnitker, Behavior of the hydrated electron at different temperatures—Structure and absorption-spectrum, *J. Phys. Chem.* **92**, 4277 (1988).
67. B. J. Schwartz and P. J. Rossky, Dynamical elements of transient spectral hole-burning of the hydrated electron, *J. Phys. Chem.* **98**, 4489 (1994).
68. B. J. Schwartz and P. J. Rossky, Aqueous solvation dynamics with a quantum-mechanical solute—Computer-simulation studies of the photoexcited hydrated electron, *J. Chem. Phys.* **101**, 6902 (1994).
69. B. J. Schwartz and P. J. Rossky, Pump-probe spectroscopy of the hydrated electron—A quantum molecular-dynamics simulation, *J. Chem. Phys.* **101**, 6917 (1994).

70. B. J. Schwartz and P. J. Rossky, Hydrated electrons as a probe of local anisotropy—Simulations of ultrafast polarization-dependent spectral hole-burning, *Phys. Rev. Lett.* **72**, 3382 (1994).

71. B. J. Schwartz and P. J. Rossky, An exploration of the relationship between solvation dynamics and spectrally determined solvent response functions by computer-simulation, *J. Phys. Chem.* **99**, 2953 (1995).

72. S. A. Egorov and B. J. Berne, Vibrational energy relaxation in the condensed phases: Quantum vs classical bath for multiphonon processes, *J. Chem. Phys.* **107**, 6050 (1997).

73. R. B. Gerber, V. Buch, and M. A. Ratner, Time-dependent self-consistent field approximation for intramolecular energy transfer. I. Formulation and application to dissociation of van der Waals molecules, *J. Chem. Phys.* **77**, 3022 (1982).

74. L. I. Schiff, *Quantum Mechanics* (McGraw–Hill, New York, 1968), 3rd ed.

75. H. Goldstein, *Classical Mechanics* (Addison–Wesley, New York, 1950), p. 273.

76. J. C. Tully, Mixed quantum-classical dynamics, *Faraday Discuss.* **110**, 407 (1998).

77. J. C. Tully, in *Modern methods for multidimensional dynamics computation in chemistry*, edited by D. L. Thompson (World Scientific, Singapore, 1998), Chapter 2.

78. F. Webster, P. J. Rossky, and R. A. Friesner, Nonadiabatic processes in condensed matter: Semiclassical theory and implementation, *Comput. Phys. Comm.* **63**, 494 (1991).

79. E. R. Bittner and P. J. Rossky, Quantum decoherence in mixed quantum-classical systems: Nonadiabatic processes, *J. Chem. Phys.* **103**, 8130 (1995).

80. D. F. Coker and L. Xiao, Methods for molecular dynamics with nonadiabatic transitions, *J. Chem. Phys.* **102**, 496 (1995).

81. S. Hammes-Schiffer, Multiconfigurational molecular dynamics with quantum transitions: Multiple proton transfer reactions, *J. Chem. Phys.* **105**, 2236 (1996).

82. K. Drukker and S. Hammes-Schiffer, An analytical derivation of MC-SCF vibrational wavefunctions for the quantum dynamical simulation of multiple proton transfer reactions: Initial application to protonated water chains, *J. Chem. Phys.* **107**, 363 (1997).

83. B. J. Austin, V. Heine, and L. J. Sham, General theory of pseudopotentials, *Phys. Rev.* **127**, 276 (1962).

84. D. F. Coker, in *Computer Simulation in Chemical Physics*, edited by M. P. Allen and D. J. Tildesley (Kluwer Academic, Dordrecht, 1993), p. 315.

85. V. Sidis, Diabatic potential energy surfaces for charge transfer processes, *Adv. Chem. Phys.* **82**, 73 (1992).

86. K. Finger and P. Saalfrank, Vibrationally excited products after the photodesorption of NO from Pt(111): A two-mode open-system density matrix approach, *Chem. Phys. Lett.* **268**, 291 (1997).

87. S. Chapman, The classical trajectory-surface-hopping approach to charge-transfer processes, *Adv. Chem. Phys.* **82**, 423 (1992).

88. S. Hammes-Schiffer and J. C. Tully, Proton transfer in solution: Molecular dynamics with quantium transitions, *J. Chem. Phys.* **101**, 4657 (1994).

89. J. C. Tully and R. K. Preston, Trajectory surface hopping approach to nonadiabatic molecular collisions: The reaction of H^+ with D_2, *J. Chem. Phys.* **55**, 562 (1971).

90. B. Space and D. F. Coker, Nonadiabatic dynamics of excited excess electrons in simple fluids, *J. Chem. Phys.* **94**, 1976 (1991).

91. B. Space and D. F. Coker, Dynamics of trapping and localization of excess electrons in simple fluids, *J. Chem. Phys.* **96**, 652 (1992).

92. K. Drukker, Ph.D. thesis, University of Amsterdam, 1998.

93. M. S. Topaler, M. D. Hack, T. C. Allison, Y. Y. Liu, S. L. Mielke, D. W. Schwenke, and D. G. Truhlar, Validation of trajectory surface hopping methods against accurate quantum mechanical dynamics and semiclassical analysis of electronic-to-vibrational energy transfer, *J. Chem. Phys.* **106**, 8699 (1997).

94. E. E. Nikitin, *Theory of Elementary Atomic and Molecular Processes in Gases* (Clarendon Press, Oxford, 1974).

95. D. Kohen, F. H. Stillinger, and J. C. Tully, Model studies of nonadiabatic dynamics, *J. Chem. Phys.* **109**, 4713 (1998).

96. U. Mueller and G. Stock, Surface-hopping modeling of photoinduced relaxation dynamics on coupled potential-energy surfaces, *J. Chem. Phys.* **107**, 6230 (1997).
97. P. Pechukas, Time-dependent semi-classical scattering theory. I. Potential scattering, *Phys. Rev.* **181**, 166 (1969).
98. P. Pechukas, Time-dependent semi-classical scattering theory. II. Atomic collisions, *Phys. Rev.* **181**, 174 (1969).
99. F. Webster, E. T. Wang, P. J. Rossky, and R. A. Friesner, Stationary phase surface hopping for nonadiabatic dynamics—2-state systems, *J. Chem. Phys.* **100**, 4835 (1994).
100. T. H. Murphrey and P. J. Rossky, Quantum dynamics simulation with approximate eigenstates, *J. Chem. Phys.* **103**, 6665 (1995).
101. Y. N. Demkov, *Variational Principles in the Theory of Collisions* (Pergamon, New York, 1963).
102. O. V. Prezhdo and P. J. Rossky, Mean-field molecular dynamics with surface hopping, *J. Chem. Phys.* **107**, 825 (1997).
103. B. J. Schwartz, E. R. Bittner, O. V. Prezhdo, and P. J. Rossky, Quantum decoherence and the isotope effect in condensed phase nonadiabatic molecular dynamics simulations, *J. Chem. Phys.* **104**, 5942 (1996).
104. M. Gell-Mann and J. B. Hartle, Classical equations for quantum-systems, *Phys. Rev. D* **47**, 3345 (1993).
105. E. R. Bittner and P. J. Rossky, Decoherent histories and nonadiabatic quantum molecular dynamics simulations, *J. Chem. Phys.* **107**, 8611 (1997).
106. O. V. Prezhdo and P. J. Rossky, Evaluation of quantum transition rates from quantum-classical molecular dynamics simulations, *J. Chem. Phys.* **107**, 5863 (1997).
107. E. J. Heller, Frozen Gaussians: A very simple semiclassical approximation, *J. Chem. Phys.* **75**, 2923 (1981).
108. E. Neria, A. Nitzan, R. N. Barnett, and U. Landmann, Quantum dynamical simulations of nonadiabatic processes: Solvation dynamics of the hydrated electron, *Phys. Rev. Lett.* **67**, 1011 (1991).
109. E. Neria and A. Nitzan, Numerical evaluation of golden-rule rates for condensed-phase processes, *Comput. Phys.* **183**, 351 (1994).
110. J. C. Alfano, P. K. Walhout, Y. Kimura, and P. F. Barbara, Ultrafast transient-absorption spectroscopy of the aqueous solvated electron, *J. Phys. Chem.* **98**, 5996 (1993).
111. Y. Kimura, J. C. Alfano, P. K. Walhout, and P. F. Barbara, Ultrafast transient absorption spectroscopy of the solvated electron in water, *J. Phys. Chem.* **98**, 3450 (1994).
112. H. J. C. Berendsen and J. Mavri, Quantum simulation of reaction dynamics by density matrix evolution, *J. Phys. Chem.* **97**, 13464 (1993).
113. N. C. Blais and D. G. Truhlar, Trajectory surface hopping study of $Na(3p^2P) + H_2 \rightarrow Na(3s^2S) + H_2(v', j', \theta)$, *J. Chem. Phys.* **79**, 1334 (1983).
114. J. Mavri and H. J. C. Berendsen, Treatment of nonadiabatic transitions by density-matrix evolution and molecular-dynamics simulations, *J. Mol. Struct.* **322**, 1 (1994).
115. J. Mavri, M. F. Lensink, and H. J. C. Berendsen, Treatment of inelastic collisions of a particle with a quantum harmonic-oscillator by density-matrix evolution, *Mol. Phys.* **82**, 1249 (1994).
116. H. J. C. Berendsen and J. Mavri, Approach to nonadiabatic transitions by density matrix evolution and molecular dynamics simulations, *Int. J. Quant. Chem.* **57**, 975 (1996).
117. M. F. Lensink, J. Mavri, and H. J. C. Berendsen, Simultaneous integration of mixed quantum-classical systems by density matrix evolution equations using interaction representation and adaptive time step integrator, *J. Comput. Chem.* **57**, 1287 (1996).
118. F. H. Long, H. Lu, and K. B. Eisenthal, Femtosecond studies of electron photodetachment of simple ions in liquid water—Solvation and geminate recombination dynamics, *J. Chem. Phys.* **91**, 4431 (1989).
119. F. H. Long, H. Lu, and K. B. Eisenthal, Femtosecond studies of the presolvated electron—An excited-state of the solvated electron, *Phys. Rev. Lett.* **64**, 1469 (1990).
120. F. H. Long, H. Lu, and K. B. Eisenthal, Femtosecond studies of electrons in liquids, *J. Opt. Soc. Am. B* **7**, 1511 (1990).
121. Y. Gauduel, A. Migus, J. L. Martin, Y. Lecarpentier, and A. Antonetti, Femtosecond optical techniques: Application to reaction dynamics in liquids, *Ber. Bunsenges. Phys. Chem.* **89**, 218 (1987).

122. A. Migus, Y. Gauduel, J. L. Martin, and A. Antonetti, Excess electrons in liquid water—1st evidence of a prehydrated state with femtosecond lifetime, *Phys. Rev. Lett.* **58**, 1559 (1987).

123. Y. Gauduel, S. Pommeret, A. Migus, and A. Antonetti, Electron reactivity in aqueous-media—A femtosecond investigation of the primary species, *Radiat. Phys. Chem.* **34**, 5 (1990).

124. Y. Gauduel, S. Pommeret, A. Migus, N. Yamada, and A. Antonetti, Femtosecond spectroscopy of an encounter pair radical (H3O+. . .e-) hyd in concentrated aqueous-solution, *J. Am. Chem. Soc.* **112**, 2925 (1990).

125. Y. Gauduel, S. Pommeret, A. Migus, and A. Antonetti, H/D isotope effects in femtosecond electron reactivity in aqueous-media, *J. Phys. Chem.* **95**, 535 (1991).

126. A. Wallqvist, D. Thirumalai, and B. J. Berne, Path integral Monte-Carlo study of the hydrated electron, *J. Chem. Phys.* **86**, 6404 (1987).

127. A. Wallqvist, G. J. Martyna, and B. J. Berne, Behavior of the hydrated electron at different temperatures—Structure and absorption-spectrum, *J. Chem. Phys.* **92**, 1721 (1988).

128. J. Schnitker and P. J. Rossky, An electron water pseudopotential for condensed phase simulation, *J. Chem. Phys.* **86**, 3471 (1987).

129. C. D. Jonah, C. Romero, and A. Rahman, Hydrated electron revisited via the Feynman path-integral route, *Chem. Phys. Lett.* **209**, 123 (1986).

130. F. Webster, J. Schnitker, M. S. Friedrichs, R. A. Friesner, and P. J. Rossky, Solvation dynamics of the hydrated electron—A nonadiabatic quantum simulation, *Phys. Rev. Lett.* **66**, 3172 (1991).

131. E. Keszei, T. H. Murphrey, and P. J. Rossky, Electron hydration dynamics—Simulation results compared to pump and probe experiments, *J. Phys. Chem.* **99**, 22 (1995).

132. J. C. Keck, Variational theory of chemical reaction rates applied to three-body recombinations, *J. Chem. Phys.* **32**, 1035 (1960).

133. J. C. Keck, Statistical investigation of dissociation cross-sections for diatoms, *Discuss. Faraday Soc.* **33**, 173 (1962).

134. C. H. Bennett, in *Algorithms for Chemical Computation*, edited by R. E. Christofferson (Amer. Chem. Soc., Washington DC, 1977).

135. J. B. Andersen, Statistical theories of chemical reactions. Distributions in the transition region, *J. Chem. Phys.* **58**, 4684 (1973).

136. S. Hammes-Schiffer and J. C. Tully, Nonadiabatic transition state theory and multiple potential energy surface molecular dynamics of infrequent events, *J. Chem. Phys.* **103**, 8528 (1995).

137. J. Montgomery, D. Chandler, and B. J. Berne, Trajectory analysis of a kinetic theory for isomerization dynamics in condensed phases, *J. Chem. Phys.* **70**, 4056 (1979).

138. J. Lobaugh and G. A. Voth, The quantum dynamics of an excess proton in water, *J. Chem. Phys.* **104**, 2056 (1996).

139. D. Li and G. A. Voth, Feynman path integral approach for studying intramolecular effects in proton transfer reactions, *J. Phys. Chem.* **95**, 10425 (1991).

140. J.-K. Hwang and A. Warshel, A quantized classical path approach for calculations of quantum-mechanical rate constants, *J. Phys. Chem.* **97**, 10053 (1993).

141. J.-K. Hwang, Z. T. Chu, A. Yadav, and A. Warshel, Simulations of quantum-mechanical corrections for rate constants of hydride-transfer reactions in enzymes and solutions, *J. Phys. Chem.* **95**, 8445 (1991).

142. J. Lobaugh and G. A. Voth, Calculation of quantum activation free-energies for proton-transfer reactions in polar solvents, *Chem. Phys. Lett.* **198**, 311 (1992).

143. J. Lobaugh and G. A. Voth, A path-integral study of electronic polarization and nonlinear coupling effects in condensed-phase proton-transfer reactions, *J. Chem. Phys.* **100**, 3039 (1994).

144. H. Azzouz and D. Borgis, A quantum molecular-dynamics study of proton-transfer reactions along asymmetrical H-bonds in solution, *J. Chem. Phys.* **98**, 7361 (1993).

145. R. Pomès and B. Roux, Quantum effects on the structure and energy of a protonated linear-chain of hydrogen-bonded water-molecules, *Chem. Phys. Lett.* **234**, 416 (1995).

146. R. Pomès and B. Roux, Theoretical study of H+ translocation along a model proton wire, *J. Chem. Phys.* **100**, 2519 (1996).

147. R. B. Gerber and M. A. Ratner, Mean-field models for molecular states and dynamics—New developments, *J. Phys. Chem.* **92**, 3252 (1988).

148. A. B. McCoy, R. B. Gerber, and M. A. Ratner, A quantitative approximation for the quantum dynamics of hydrogen-transfer—Transition-state dynamics and decay in C1HCl-, *J. Chem. Phys.* **101**, 1975 (1994).

149. R. Alimi, R. B. Gerber, A. D. Hammerich, R. Kosloff, and M. A. Ratner, Validity of time-dependent self-consistent-field (tdscf) approximations for uni-molecular dynamics—A test for photodissociation of the Xe-Hl cluster, *J. Chem. Phys.* **93**, 6484 (1990).

150. A. García-Vela, R. B. Gerber, and J. J. Valentini, Effects of solvation by a single atom in photodissociation—Classical and quantum classical-studies of HCl photolysis in Ar. . .HCl, *J. Chem. Phys.* **97**, 3297 (1992).

151. A. Garcíia-Vela, R. B. Gerber, and D. G. Imre, Mixed quantum wave packet classical trajectory treatment of the photodissociation process $ArHCl \rightarrow Ar + H + Cl$, *J. Chem. Phys.* **97**, 7242 (1992).

152. P. Bala, P. Grochowski, B. Lesyng, and J. A. McCammon, Quantum-classical molecular dynamics simulations of proton transfer processes in molecular complexes and in enzymes, *J. Phys. Chem.* **100**, 2535 (1996).

153. N. Makri, Time-dependent self-consistent field approximation with explicit two-body correlations, *Chem. Phys. Lett.* **169**, 541 (1990).

154. N. Makri and W. H. Miller, Time-dependent self-consistent field (TDSCF) approximation for a reaction coordinate coupled to a harmonic bath—Single and multiple configuration treatments, *J. Chem. Phys.* **87**, 5781 (1987).

155. Z. Kotler, A. Nitzan, and R. Kosloff, Multiconfiguration time-dependent self-consistent field approximation for curve crossing in presence of a bath—A fast Fourier-transform study, *Chem. Phys. Lett.* **153**, 483 (1988).

156. H.-D. Meyer, U. Manthe, and L. S. Cederbaum, The multi-configurational time-dependent Hartree approach, *Chem. Phys. Lett.* **165**, 73 (1990).

157. U. Manthe, H.-D. Meyer, and L. S. Cederbaum, Wave-packet dynamics within the multiconfiguration Hartree framework: General aspects and application to NOCI, *J. Chem. Phys.* **97**, 3199 (1992).

158. U. Manthe, H.-D. Meyer, and L. S. Cederbaum, Multiconfigurational time-dependent Hartree study of complex dynamics: Photodissociation of NO2, *J. Chem. Phys.* **97**, 9062 (1992).

159. A. D. Hammerich, R. Kosloff, and M. A. Ratner, Quantum-mechanical reactive scattering by a multiconfigurational time-dependent self-consistent field (mctdscf) approach, *Chem. Phys. Lett.* **171**, 97 (1990).

160. Z. Kotler, E. Neria, and A. Nitzan, Multiconfiguration time-dependent self-consistent field approximations in the numerical-solution of quantum dynamic problems, *Comput. Phys. Comm.* **63**, 243 (1991).

161. A. P. J. Jansen, A multiconfiguration time-dependent Hartree approximation based on natural single-particle states, *J. Chem. Phys.* **99**, 4055 (1993).

162. J.-Y. Fang and H. Guo, Multiconfiguration time-dependent Hartree studies of the Cl2Ne vibrational predissociation dynamics, *J. Chem. Phys.* **102**, 1944 (1995).

163. A. D. Hammerich, U. Manthe, R. Kosloff, H.-D. Meyer, and L. S. Cederbaum, Time-dependent photodissociation of methyl-iodine with 5 active modes, *J. Chem. Phys.* **101**, 5623 (1994).

164. U. Manthe and A. D. Hammerich, Wavepacket dynamics in five dimensions. Photodissociation of methyl iodide, *Chem. Phys. Lett.* **211**, 7 (1993).

165. J. Campos-Martínez and R. D. Coalson, Adding configuration interaction to the time-dependent Hartree grid approximation, *J. Chem. Phys.* **93**, 4740 (1990).

166. J. Campos-Martínez, J. R. Waldeck, and R. D. Coalson, Beyond the time-dependent Hartree grid approximation for curve-crossing problems, *J. Chem. Phys.* **96**, 3613 (1992).

167. B. Vekhter, M. A. Ratner and R. B. Gerber, Dynamic mean-field models with correlated modes, *J. Chem. Phys.* **99**, 7916 (1993).

168. R. B. Gerber and R. Alimi, Quantum molecular-dynamics by a perturbation-corrected time-dependent self-consistent-field method, *Chem. Phys. Lett.* **184**, 69 (1991).

169. A. Szabo and N. S. Ostlund, *Modern Quantum Chemistry, Introduction to Advanced Electronic Structure Theory* (McGraw–Hill, New York, 1982).

170. J. K. Cullum and R. A. Willoughby, *Lanczos Algorithms for Large Symmetric Eigenvalue Computations* (Birkhauser, Boston, 1985).

171. A. Askar and A. S. Cakmak, Explicit integration method for the time-dependent Schroedinger equation for collision problems, *J. Chem. Phys.* **68**, 2794 (1978).

172. H. Tal-Ezer and R. Kosloff, An accurate and efficient scheme for propagation of the time-dependent Schroedinger equation, *J. Chem. Phys.* **81**, 3967 (1984).

173. M. Sprik and M. L. Klein, Optimization of a distributed Gaussian basis set using simulated annealing—Application to the solvated electron, *J. Chem. Phys.* **87**, 5987 (1987).

174. R. Kosloff, Time-dependent quantum-mechanical methods for molecular dynamics, *J. Phys. Chem.* **92**, 2087 (1988).

175. R. N. Barnett, U. Landman, and A. Nitzan, Dynamics and spectra of a solvated electron in water clusters, *J. Phys. Chem.* **89**, 2242 (1988).

176. P. Pulay, Ab initio calculation of force constants and equilibrium geometries in polyatomic molecules. I. Theory, *Mol. Phys.* **17**, 179 (1969).

177. P. Pulay, in *Modern Theoretical Chemistry, Vol. 4, Applications of Electronic Structure Theory*, edited by H. F. Schaefer III (Plenum Press, New York, 1977), p. 153.

178. J. Hinze, MC-SCF. I. The multi-configurational self-consistent-field method, *J. Chem. Phys.* **59**, 6424 (1973).

179. D. M. Blow, Structure and mechanism of Chymotrypsin, *Acc. Chem. Res.* **9**, 145 (1976).

180. G. Zundel, Proton-transfer in and proton polarizability of hydrogen-bonds—IR and theoretical-studies regarding mechanisms in biological-systems, *J. Mol. Struct.* **177**, 43 (1988).

181. S. Ramaswamy, H. Eklund, and B. V. Plapp, Structures of horse liver alcohol dehydrogenase complexed with NAD+ and substituted benzyl alcohols, *Biochemistry* **33**, 5230 (1994).

182. X. Ren, C. K. Tu, P. J. Laipis, and D. N. Silverman, Proton-transfer by histidine-67 in site-directed mutants of human carbonic-anhydrase-III, *Biochemistry* **34**, 8492 (1995).

183. R. A. Mathies, S. W. Lin, J. B. Ames, and W. T. Pollard, From femtoseconds to biology—Mechanism of bacteriorhodopsins light-driven proton pump, *Annu. Rev. Biophys. Biophys. Chem.* **20**, 491 (1991).

184. R. Henderson, Model for the structure of Bacteriorhodopsin based on high-resolution electron cryomicroscopy, *J. Mol. Biol.* **213**, 899 (1990).

185. M. Y. Okamura and G. Feher, Proton-transfer in reaction centers from photosynthetic bacteria, *Annu. Rev. Biochem.* **61**, 861 (1992).

186. L. Baciou and H. Michel, Interruption of the water chain in the reaction-center from rhodobacter-sphaeroides reduces the rates of the proton uptake and of the 2nd electron-transfer to Q(B), *Biochemistry* **34**, 7967 (1995).

187. R. Pomès and B. Roux, Theoretical study of the structure and dynamics of biological proton wires, *Biophys. J* **71**, 670 (1996).

188. M. Morillo and R. I. Cukier, On the effects of solvent and intermolecular fluctuations in proton-transfer reactions, *J. Chem. Phys.* **92**, 4833 (1990).

189. A. Suárez and R. Silbey, Hydrogen tunneling in condensed media, *J. Chem. Phys.* **94**, 4809 (1991).

190. A. Warshel and Z. T. Chu, Quantum corrections for rate constants of diabatic and adiabatic reactions in solutions, *J. Chem. Phys.* **93**, 4003 (1990).

191. J. Aqvist and A. Warshel, Simulation of enzyme-reactions using valence-bond force-fields and other hybrid quantum-classical approaches, *Chem. Rev.* **93**, 2523 (1993).

192. D. G. Truhlar, Y.-P. Liu, G. K. Schenter, and B. C. Garrett, Tunneling in the presence of a bath—A generalized transition-state theory approach, *J. Phys. Chem.* **98**, 8396 (1994).

193. D. Borgis, G. Tarjus, and H. Azzouz, Solvent-induced proton-transfer in strongly H-bonded complexes—An adiabatic dynamic simulation study, *J. Phys. Chem.* **96**, 3188 (1992).

194. D. Borgis, G. Tarjus, and H. Azzouz, An adiabatic dynamic simulation study of the Zundel polarization of strongly H-bonded complexes in solution, *J. Phys. Chem.* **97**, 1390 (1992).

195. D. Laria, G. Ciccotti, M. Ferrario, and R. Kapral, Molecular-dynamics study of adiabatic proton-transfer reactions in solution, *J. Chem. Phys.* **97**, 378 (1992).

196. D. Borgis and J. T. Hynes, Dynamic theory of proton tunneling transfer rates in solution—General formulation, *Computers Phys.* **170**, 315 (1993).

197. J. Mavri, H. J. C. Berendsen, and W. F. van Gunsteren, Influence of solvent on intramolecular proton-transfer in hydrogen halonate—Molecular dynamics simulation study of tunneling by density-matrix evolution and nonequilibrium solvation, *J. Phys. Chem.* **97**, 13469 (1993).

198. J. Mavri and H. J. C. Berendsen, Calculation of the proton-transfer rate using density matrix evolution and molecular dynamics simulations—Inclusion of the proton excited states, *J. Chem. Phys.* **99**, 12711 (1995).

199. A. Staib, D. Borgis, and J. T. Hynes, Proton-transfer in hydrogen-bonded acid–base complexes in polar-solvents, *J. Chem. Phys.* **102**, 2487 (1995).

200. K. Ando and J. T. Hynes, HCl acid ionization in water—A theoretical molecular modeling, *J. Mol. Liq.* **64**, 25 (1995).

201. P. Bala, B. Lesyng, and J. A. McCammon, Applications of quantum-classical and quantum-stochastic molecular dynamics simulations for proton transfer processes, *Comput. Phys.* **180**, 271 (1994).

202. S. Hammes-Schiffer and J. C. Tully, Vibrationally enhanced proton-transfer, *J. Chem. Phys.* **99**, 5793 (1995).

203. M. Tuckerman, K. Laasonen, M. Sprik, and M. Parrinello, Ab-initio molecular-dynamics simulation of the solvation and transport of hydronium and hydroxyl ions in water, *J. Chem. Phys.* **103**, 150 (1995).

204. X. Duan and S. Scheiner, Analytic-functions fit to proton-transfer potentials, *J. Mol. Struct.* **270**, 173 (1992).

205. H.-P. Cheng, R. N. Barnett, and U. Landman, All-quantum simulations—H3O+ and H502+, *Chem. Phys. Lett.* **237**, 161 (1995).

206. C. Kobayashi, K. Iwahashi, S. Saito, and I. Ohmine, Dynamics of proton attachment to water cluster: Proton transfer, evaporation, and relaxation, *J. Chem. Phys.* **105**, 6358 (1996).

207. K. Drukker, S. W. de Leeuw, and S. Hammes-Schiffer, Proton transport along water chains in an electric field, *J. Chem. Phys.* **108**, 6799 (1998).

208. H. Decornez, K. Drukker, M. M. Hurley, and S. Hammes-Schiffer, Proton transport along water chains and NADH hydride transfer in solution, *Ber. Bunsen. Ges. Phys. Chem.* **102**, 533 (1998).

209. S. Hammes-Schiffer, in *Advances in Classical Trajectory Methods*, edited by W. S. Hase (JAI Press, Stamford, CT, 1998), p. 73.

210. F. H. Stillinger and C. W. David, Polarization model for water and its ionic dissociation products, *J. Chem. Phys.* **69**, 1473 (1978).

211. F. H. Stillinger, Dynamics and ensemble averages for the polarization models of molecular interactions, *J. Chem. Phys.* **71**, 1647 (1979).

212. T. A. Weber and F. H. Stillinger, Reactive collisions of hydronium and hydroxide ions studied with the polarization model, *J. Phys. Chem.* **86**, 1314 (1982).

213. H. Decornez, K. Drukker, and S. Hammes-Schiffer, Hydrogen-bonding and solvation effects on proton wires, *J. Phys. Chem. A* **103**, 2891 (1999).